



Trigger factor is a *bona fide* secretory pathway chaperone that interacts with SecB and the translocase

Jozefien De Geyter[†], Athina G Portaliou[†], Bindu Srinivasu, Srinath Krishnamurthy, Anastassios Economou^{*}  & Spyridoula Karamanou^{**} 

Abstract

Bacterial secretory preproteins are translocated across the inner membrane post-translationally by the SecYEG-SecA translocase. Mature domain features and signal peptides maintain preproteins in kinetically trapped, largely soluble, folding intermediates. Some aggregation-prone preproteins require chaperones, like trigger factor (TF) and SecB, for solubility and/or targeting. TF antagonizes the contribution of SecB to secretion by an unknown molecular mechanism. We reconstituted this interaction *in vitro* and studied targeting and secretion of the model preprotein pro-OmpA. TF and SecB display distinct, unsuspected roles in secretion. Tightly associating TF:pro-OmpA targets the translocase at SecA, but TF prevents pro-OmpA secretion. In solution, SecB binds TF:pro-OmpA with high affinity. At the membrane, when bound to the SecA C-tail, SecB increases TF and TF:pro-OmpA affinities for the translocase and allows pro-OmpA to resume translocation. Our data reveal that TF, a main cytoplasmic folding pathway chaperone, is also a *bona fide* post-translational secretory chaperone that directly interacts with both SecB and the translocase to mediate regulated protein secretion. Thus, TF links the cytoplasmic folding and secretion chaperone networks.

Keywords outer membrane protein A; protein targeting; SecB; Sec system; trigger factor

Subject Categories Membrane & Trafficking; Translation & Protein Quality

DOI 10.15252/embr.201949054 | Received 16 August 2019 | Revised 9 March 2020 | Accepted 19 March 2020 | Published online 19 April 2020

EMBO Reports (2020) 21: e49054

Introduction

In post-translational, Sec-dependent secretion ribosome-released nascent polypeptide chains delay their folding for the duration of their cytoplasmic transit [1] and resume it in distinct cellular

locations on the *trans* side of the membrane [2]. A total of 505 different proteins, carrying signal peptides (SPs) fused N-terminally to their mature domains, follow this process in *Escherichia coli* (*E. coli*) K-12 [1,3–6]. Secretion occurs through an inner membrane channel (~2.5 nm) formed by the SecYEG proteins [7]. Translocation starts once SecA, an ATPase motor that shuttles between cytoplasm and membrane, peripherally associates with SecYEG [8], and the preprotein binds bivalently onto SecA, *via* both its SP and its mature domain [1,2,9,10].

Secretory proteins constitute a novel protein class with enhanced disorder, reduced hydrophobicity and aggregation propensity [6,11–13]. Their unusual structural features directly impact the membrane targeting process. Most of them form slow-folding intermediates that can remain soluble for long, *in vitro* [11]. This may render them largely independent of chaperones or SPs, both previously thought essential for maintaining them unfolded thus allowing targeting and translocation competence [14–19], even *in vivo* [9,11]. Slow folding, with or without chaperones, exposes mature domain targeting signals (MTSs) [9] that mediate targeting to the translocase with nanomolar affinity and allow export [9,20,21].

Chaperones are often abundant in cells, some of them particularly under stress [17] and can occupy strategic locations, e.g. bound to the ribosome or in the periplasm. A balanced cooperation of chaperone networks is essential for cell viability [22]. Two chaperones proposed to have specific roles in protein secretion in *E. coli* K-12 are as follows: (i) the tetrameric SecB. Found only in some proteobacteria [23], it is proposed to be the main secretory pathway chaperone since it binds unfolded preproteins and interacts with SecA [24], *via* complexing the C-terminal tail of the latter with low micromolar affinity [25]. Yet, SecB clients in *E. coli* may be ~20 [1]. (ii) Trigger factor (TF), a ubiquitous cytoplasmic dimer and ribosome-bound monomer, commonly facilitates folding of cytoplasmic folder clients or hands them over to downstream foldases such as DnaK and GroEL [26,27]. TF has been circumstantially implicated in the secretory pathway due to its interaction with ~20% of nascent secretory polypeptides at the ribosomal exit tunnel [6]. *In vitro*, TF maintains the translocation competence of secretory polypeptides

Department of Microbiology and Immunology, Rega Institute for Medical Research, Laboratory of Molecular Bacteriology, KU Leuven, Leuven, Belgium

^{*}Corresponding author. Tel: +32 16 37 92 73; E-mail: tassos.economou@kuleuven.be

^{**}Corresponding author. Tel: +32 16 37 92 08; E-mail: lily.karamanou@kuleuven.be

[†]These authors contributed equally to this work

like pro-OmpA [28,29] and solubilizes 19 aggregation-prone secretory proteins [6,30].

Due to its high intracellular concentration ($\sim 40 \mu\text{M}$ TF; Appendix Table S1 at [1]), TF is commonly bound to ribosomes (concentration $\sim 20 \mu\text{M}$ [1,31]) because of its $\sim 1 \mu\text{M}$ K_d for them [27,32]. It patrols the ribosome exit tunnel [33,34] and contributes, together with other ribosome-bound factors, to the folding and sorting of cytoplasmic proteins [27] and the sorting of co- and post-translationally targeted secretory proteins [32,35–37] through an interplay with the signal recognition particle [32,36] and with ribosome-bound SecA [38]. TF protects hydrophobic regions of secretory nascent chains [28,33,39] using four hydrophobic patches per monomer [16]. However, TF is not essential for *in vivo* secretion [40] and its precise role in preprotein sorting, targeting and solubilization remains elusive.

SecB, a dimer of dimers, interacts with secretory chains [41] via a long hydrophobic groove along a surface formed by all its protomers and undergoes slight conformational changes upon binding to secretory preproteins [42]. SecB prevents or delays preprotein folding and may relay preproteins to cytoplasmic or SecYEG-bound SecA [43,44]. Initiation of ATP hydrolysis by SecA causes SecB release [1,43].

K-12 cells devoid of SecB [22,45], TF [22] or both [22] are viable although SecB or TF deletion causes some increase in intracellular protein aggregation [46], compromised cell division [40] and transcriptome alterations [47]. This cellular adaptation to their absence has been attributed to the built-in redundancy of chaperone networks [48]. In the absence of TF and SecB, more ribosomes become membrane-associated and translocation may become more co-translational [22,49]. At low temperatures, deletion of *secB* causes lethality; this phenotype is restored if additionally, the TF-encoding *tig* gene is deleted [22]. Apparently, high intracellular TF concentration is not tolerated for certain clients depending on their affinities; relief by SecB suggests that some of them might be secretory. TF has been previously shown to slow down protein secretion [50]. These observations suggested that TF and SecB may somehow cooperate in post-translational protein export [22,50].

Non-ATPase chaperones like TF and SecB are thought to act primarily as holdases [42,51–54]; i.e., they would bind and remain bound onto a secretory chain with a low k_{off} until the latter is delivered to the translocase [16,42]. Both TF and SecB can also bind preproteins [16,42] that do not need chaperones for solubility, targeting and secretion [9,11].

We investigated the independent roles and functions of TF and SecB and their potential cooperation in preprotein targeting and translocation. We studied the type and affinity of the interactions between TF, SecB and the model secretory protein pro-OmpA (outer membrane protein A). The conformation of non-folded pro-OmpA was previously analysed using biophysical tools including hydrogen–deuterium exchange-mass spectrometry (HDX-MS) [11]. It contains substantial secondary but no tertiary structure and is soluble under reducing conditions [11,55]. The OmpA mature domain will only fold after insertion in the outer membrane [56].

Our data reveal that both TF and SecB interact with pro-OmpA but differently. TF acting as a tight and SecB as a weak pro-OmpA holdase can sequester it away, thereby avoiding the formation of off-pathway, translocation-incompetent states. Tightly associating TF:pro-OmpA complexes do arrive at the Sec translocase, but pro-

OmpA is not released for secretion. Three new SecB roles were revealed as follows: (i) it complexes TF:pro-OmpA in solution; (ii) it increases the individual TF and TF:pro-OmpA affinities for the translocase, and (iii) it acts as a release factor at the translocase for TF-bound pro-OmpA by binding to the C-tail of SecA. These multi-level roles may explain why balanced TF:SecB ratios are essential for viability. These previously unknown TF interactions with SecB and the translocase place TF on the post-translational secretory pathway ushering a subset of secretory proteins.

Results

An optimal SecB/TF ratio is essential *in vivo*

The ratio of SecB to TF is maintained optimal *in vivo* [22,50]. This requirement is so important that even in wild-type MC4100 cells, elevated synthesis of TF *in trans* in the presence of the transcriptional inducer of the tetracycline-activated promoter anhydrotetracycline (AHT) leads to either lethality (Fig 1A, 16°C; compare row 2 to row 1) or to a severe growth defect (30°C). Correspondingly, strain MC4100 Δ *secB* that produces TF in the absence of SecB displays lethality at the non-permissive temperature of 16°C (Fig 1A, row 3), but this is corrected by either expressing *secB* in *trans* from a plasmid (row 4) or by additionally deleting the *tig* gene that encodes TF (row 5) [22]. If in this otherwise completely viable strain MC4100 Δ *tig* Δ *secB*, *tig* is expressed *in trans* from a plasmid, lethality is re-capitulated in the presence of AHT but also, to a lesser extent, in its absence (row 6). The effect is so severe that in *trans*, TF synthesis becomes lethal even at the otherwise permissive temperature of 30°C (row 6, right).

To identify TF regions important for inhibition, we used the composite derivative *tig* (4A,3A) in which two main functional regions of TF are compromised by alanine mutagenesis: its client binding site region 2 (4A: M374A, Y378A, V384A and F387A) [51] and its ribosome binding domain (3A: F44A, R45A and K46A) [57] and *tig*(4A,3A) no longer inhibit viability (Fig 1A, lane 7). Using the individually mutated derivatives 4A and 3A that are compromised for client [51] and ribosome [57] binding affinities, respectively, we determined that TF-mediated growth inhibition requires primarily optimal client (lane 8; *tig*(4A)) and much less so ribosome (lane 9; *tig*(3A)) association. All TF derivatives remained stable and detectable in similar amounts (Fig EV1A).

Based on the above, we hypothesized that excess of TF might sequester away some critical secretory proteins, downstream of its ribosome-associated state, and thus, becomes deleterious for the secretory pathway. We presumed that SecB might antagonise, directly or indirectly, this tight TF association with secretory clients. To probe this hypothesis, we reconstituted the reaction *in vitro*.

SecB relieves TF-inhibited translocation of pro-OmpA *in vitro*

To investigate the deleterious effect of TF, we used an *in vitro* preprotein translocation assay. pro-OmpA, retained non-folded in chaotrope, was diluted into an aqueous buffer in the absence (Fig 1B, I and II) or presence (III and IV) of Sec pathway components. We previously established that under these assay conditions, preproteins commonly retain their non-folded, soluble structures for

long [11]. Hence, we were able to study under one regime their structural dynamics, using hydrogen–deuterium exchange-mass spectrometry (HDX-MS) (Fig 1B and I) [10,11], as well as their

functional interaction with chaperones like TF and SecB (Fig 1B, II), or/and with the SecYEG-SecE translocase (Fig 1B, III). Addition of the latter, in inverted inner membrane vesicles (IMVs) that had been

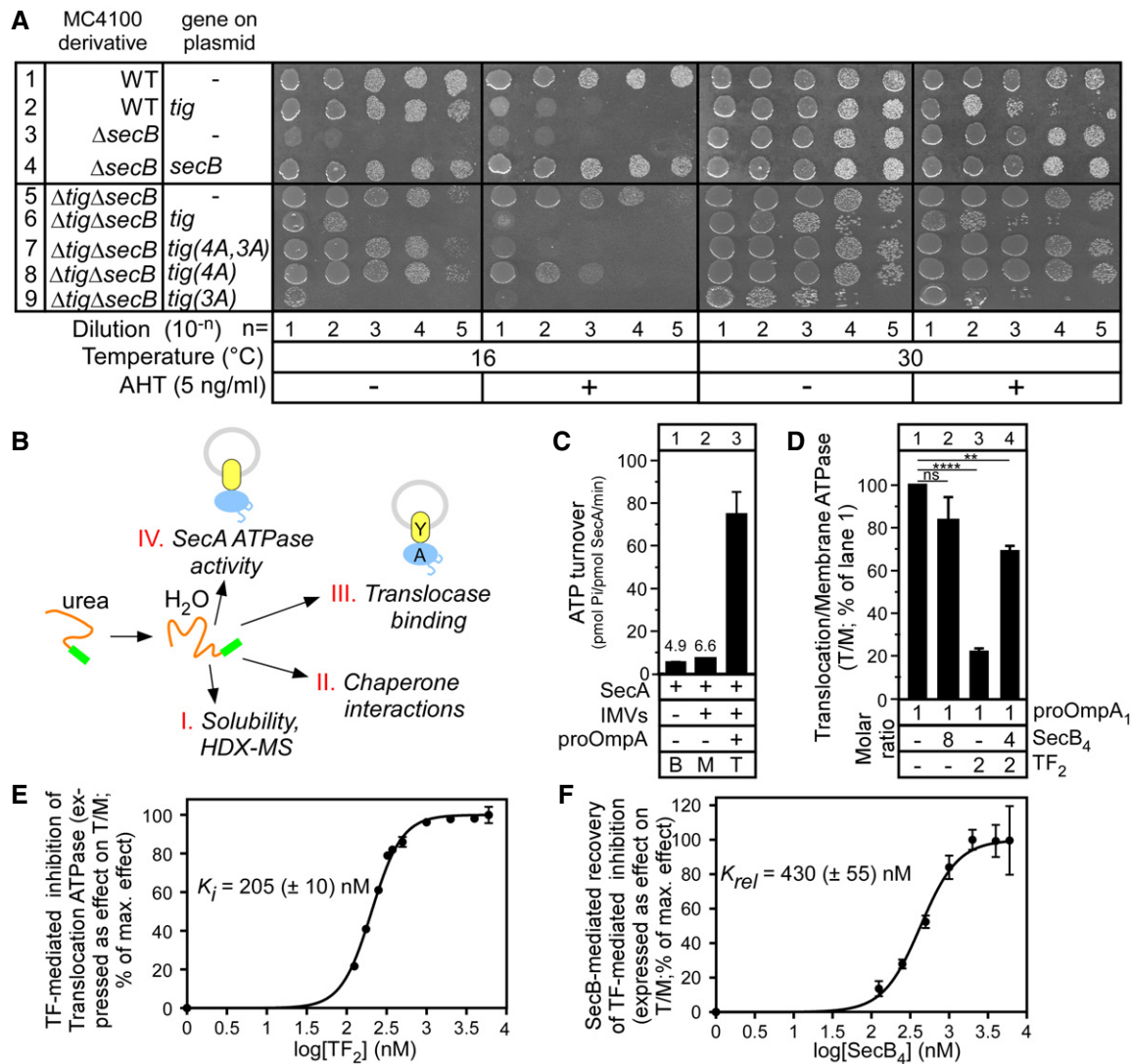


Figure 1. An optimal TF/SecB ratio is essential for cell viability and *in vitro* translocation of pro-OmpA.

A *In vivo* genetic complementation of the *E. coli* MC4100 wild-type (WT) and *secB* or/and *tig* knock-out derivatives by either an empty vector or one carrying the *secB* or *tig* (encoding TF) genes or derivatives (see "Plasmid" table in Appendix), as indicated. Serial dilutions of a culture ($OD_{600} = 0.5$) were spotted (12 μ l) on LB-Ampicillin plates containing or not anhydrotetracycline (AHT; 5 ng/ml) and grown at 16 $^{\circ}C$ or 30 $^{\circ}C$ (as indicated). $n = 3-7$ biological replicates.

B Schematic summary of the assays used in this study. Preproteins (purified commonly in 6 M urea; except in Appendix Fig S6B) were diluted in an aqueous buffer (final urea < 0.2 M) and their physicochemical properties and functional interactions with Sec system components analysed. Y: SecYEG; A: SecA.

C SecA ATPase activity determination in solution (basal; B), or plus SecYEG IMVs; (membrane; M) or plus pro-OmpA (pre-treated with 10 mM DTT; 5 mM EDTA; 20 min; 4 $^{\circ}C$; translocation; T). $n = 21$ biological replicates. Mean values (\pm SEM) are shown.

D pro-OmpA translocation ATPase activity stimulation of SecA (as in C) in the absence or presence of TF₂ or/and SecB₄, added at the indicated molar excess over pro-OmpA₁. The T/M ratios were calculated; the one in the absence of chaperones was considered as 100%, and all other values were expressed as % of this. $n = 2-4$ biological replicates. Mean values (\pm SEM) are shown. Unpaired parametric t-test, 95% confidence interval: ns: not significant ($P = 0.1032$); **** $P < 0.0001$; ** $P = 0.0037$.

E Titrated TF-mediated inhibition (0–6 μ M range) of pro-OmpA-stimulated translocation ATPase activity (as in C). Values were normalized (effect_{max} = 100%; effect_{min} = 0%) and plotted ($n = 1-4$ biological replicates; mean values \pm SEM) versus the $\log_{10}[TF_2]$. The K_i was determined using a variable slope fit ($\log[\text{inhibitor}]$ versus normalized response; GraphPad Prism).

F SecB-mediated relief of TF-mediated inhibition of pro-OmpA translocation ATPase activity (as in C). TF₂ (1 μ M) and SecB₄ (0–6 μ M) were used. The T/M ratios were calculated, normalized (as in D) and plotted ($n = 2-3$ biological replicates; mean values \pm SEM) versus the $\log_{10}[SecB_4]$. An apparent relief constant (K_{rel}) was determined (as in E).

Source data are available online for this figure.

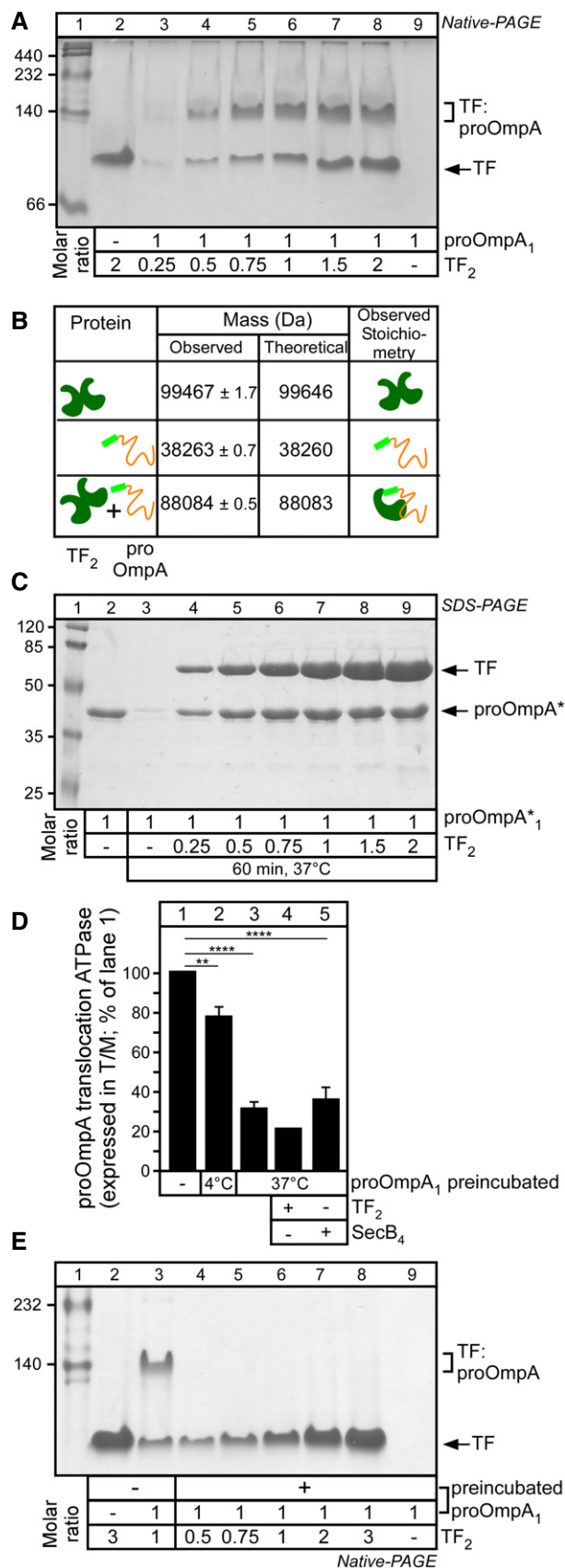


Figure 2. TF is a tight holdase for translocation-competent pro-OmpA.

- A** TF–pro-OmpA physical interaction in solution. pro-OmpA₁ (5 μM) was incubated (50 μl; Buffer C; < 0.2 M urea; 37°C; 60 min) with the indicated molar excess of TF₂. Soluble proteins were analysed on 10% native-PAGE (4 mA; 16 h; 4°C) and Coomassie Blue stained. A representative experiment is shown; *n* = 4 biological replicates.
- B** TF–pro-OmpA intact native-MS analysis. Mass spectra of TF₂ (20 μM; Buffer G), pro-OmpA (20 μM; pre-treated with 10 mM DTT; Buffer G) or their mixture were acquired in near-native conditions using a Synapt G2 mass spectrometer and analysed using MassLynX 4.1, and masses were deconvoluted using MaxEnt 1 and shown together with the theoretical masses and deduced stoichiometries. *n* = 2 biological replicates.
- C** TF solubilizes pro-OmpA*. pro-OmpA*₁ (5 μM) was incubated (50 μl; Buffer C; < 0.2 M urea; 37°C; 60 min) alone or in the presence of TF. Proteins in the soluble fraction were analysed on 15% SDS–PAGE and Coomassie Blue stained. Lane 2: 2.84 μg pro-OmpA*. Representative experiment is shown; *n* = 5 biological replicates.
- D** pro-OmpA pre-incubated at 37°C fails to stimulate SecA ATPase activity. pro-OmpA (0.5 μM) was either diluted directly (lane 1) or after preincubation alone (10 min; Buffer D; < 0.2 M urea; either at 4°C or 37°C) into reactions containing SecYEG–SecA alone or together with TF₂ or SecB₄ (2 and 4× molar excess over pro-OmpA, respectively). T/M ratios (as in Fig 1D) are shown (*n* = 8 biological replicates; mean values ± SEM; unpaired parametric *t*-test, 95% confidence interval: ***P* = 0.0017; *****P* < 0.0001).
- E** pro-OmpA pre-incubated at 37°C does not interact with TF. pro-OmpA₁ (5 μM) was pre-incubated (Buffer D; < 0.2 M urea; 37°C; 10 min) or not (lane 3), prior to addition of the indicated molar excess of TF₂ (analysed as in A). Representative experiment is shown; *n* = 4 biological replicates.

Source data are available online for this figure.

urea-stripped of any peripheral components, allowed us to study the effect of soluble factors added *in trans* on either docking onto the translocase (Fig 1B, III) or on the ability of SecA to hydrolyse ATP (Fig 1B, IV) [10,58].

We first monitored ATP turnover by SecA (Fig 1B, IV) as it catalyses protein translocation (Fig 1C) [58]. The low-level basal ATPase activity of SecA [basal (B) ATPase, lane 1] is stimulated ~1.4-fold by the addition of SecYEG-containing IMVs (membrane (M) ATPase, lane 2) and a further ~11-fold when pro-OmpA is diluted from 6 M to 0.12 M urea into the reaction (translocation (T) ATPase, lane 3). Equimolar SecYEG–SecA ratios were used (0.4 μM), and following titration experiments (Fig EV1B, lane 3), pro-OmpA was added at 0.5 μM, the maximal concentration that still yields a linear range of ATPase stimulation.

Similar experiments were performed in the presence of TF and SecB, added alone or together. Since TF or SecB has no effect on the basal or membrane ATPase of SecA (Fig EV1C), we focused on the translocation ATPase. To compare across the different conditions, the ratio of translocation to membrane ATPase (T/M) in the absence of TF or SecB (Fig 1C, lanes 2–3) was considered as 100% and all other ratios were expressed as a percent of this value (Fig 1D, lanes 1–4). Addition of SecB alone had no adverse effect on translocation ATPase activity (lane 2). In contrast, the presence of TF led to extensive inhibition of pro-OmpA-stimulated translocation ATPase activity (lane 3) that was significantly relieved when SecB was also present (lane 4). The TF-mediated repression of translocation ATPase was specific to pro-OmpA, a known preferred TF client [28,39,51], and was not observed with other preproteins to which TF also binds *in vitro* (e.g. pro-PhoA; Fig EV1D).

We titrated the effect of TF, using 0–6 μM TF dimer (TF₂, the native quaternary state), on the translocation ATPase of SecA, yielding a K_i of 205 (\pm 10) nM (Fig 1E), suggesting high-affinity binding of TF for pro-OmpA.

Next, we titrated the effect of SecB, using 0–6 μM SecB tetramer (SecB₄, the native quaternary state), on the inhibition of the translocation ATPase caused by 1 μM of TF. The effect of SecB on the T/M ratio was determined, normalized (effect_{max} = 100%) and plotted against the log-transformed SecB₄ concentration. Using the same fit as before, we determined a relief constant (K_{rel}) of 425 (\pm 10) nM (Fig 1F) that suggested high-affinity binding of SecB₄ with either TF: pro-OmpA or the SecYEG-SecA translocase (see below). SecB₄ binds to the latter with an affinity of 200–330 nM (Fig EV1E) [44].

Presumably, TF binding either prevents pro-OmpA from being targeted to the translocase or, post-targeting, it prevents pro-OmpA from being translocated. SecB might act at either one of these steps.

Tight binding of TF to pro-OmpA

We further probed TF complex formation with pro-OmpA, first using native-PAGE (Fig 2A). Unlike TF (Fig 2A, lane 2; apparent mass \sim 100 kDa), non-folded pro-OmpA is not resolved by native-PAGE as a sharp band (lane 9). However, addition of increasing molar excess of TF₂ to pro-OmpA resulted in increasing formation of a species migrating slower than TF, indicative of complex formation (lanes 3–8).

TF self-dimerizes with an affinity of \sim 1.5–2 μM [59] (Appendix Fig S1) yielding a mass determined by native-mass spectrometry (native-MS) of 99,467 \pm 1.7 Da (Fig 2B). Binding to pro-OmpA (mass of 38,263 \pm 0.7 Da) yields a TF:pro-OmpA complex of 88,084 \pm 0.5 Da, consistent with a 1:1 stoichiometry (Fig 2B; Appendix Fig S2). 1:1 stoichiometry was also reported for TF:pro-PhoA [16].

TF binding prevents pro-OmpA from aggregating

Next, we probed the ability of TF to prevent pro-OmpA aggregation (Fig 1B, II). For this specific assay, we resorted to using pro-OmpA*, an aggregation-prone derivative (Appendix Fig S1B) [11], incubated under conditions that maximally promote its aggregation (5 μM ; 60 min at 37°C; without DTT/EDTA pre-treatment; Fig EV1F) in the absence (Fig 2C, lane 3) or presence of TF (lanes 4–9). Insoluble material was removed by centrifugation before soluble supernatants were analysed by SDS-PAGE and native-PAGE, Coomassie Blue staining and densitometry. While pro-OmpA* alone aggregated extensively (Fig 2C, compare lanes 2 and 3; Appendix Fig S3), its solubility increased in a TF concentration-dependent manner (lanes 4–9).

We concluded that TF association can prevent pro-OmpA aggregation by forming a stable complex corroborating previous data [28,29].

TF does not associate with off-pathway pro-OmpA folding intermediates

pro-OmpA that is diluted into aqueous buffer and incubated for 10 min at 4°C before being added to SecYEG-SecA (Fig 2D, lane 2) is slightly less efficient in stimulating SecA translocation ATPase from the same protein that is diluted in the presence of SecYEG-

SecA (compare lane 2 to 1). Moreover, if pro-OmpA is incubated for 10 min at 37°C prior to its addition to SecYEG-SecA, a 70–80% loss of stimulation was detected (lane 3). Aggregation, that could justify this loss of activity, was not observed (Appendix Fig S1C). We therefore presumed that acquisition of off-pathway folding intermediates, similar to the ones we previously detected [11], might be responsible for reduced translocation ATPase stimulation.

To test this directly, we monitored pro-OmpA folding kinetics (at 4°C and 37°C), by global HDX-MS analysis [11,60], and in the same course of time, we followed its ability to stimulate the translocation ATPase of SecA (Fig EV2A and B, respectively). At 4°C, within 1–10 min, pro-OmpA acquires two intermediates that take up less deuterium (D) than the fully deuterated (FD) control, i.e. are more folded (I₁ and I₂; Fig EV2A, middle; compare to FD on top) and which remain on-pathway for translocation for 60 min as judged by the T/M ratio (Fig EV2B, middle). In contrast, at 37°C pro-OmpA rapidly shifts to a single intermediate, detectable for at least 1 h, that takes up less D than I₁ yet more than I₂ (Fig EV2A, bottom) and which rapidly loses the ability to stimulate translocation ATPase (Fig EV2B, bottom). Once the I₃ intermediate was preformed (10 min; aqueous buffer; 37°C; Fig EV2A, bottom), mixing it with TF did not lead to complex formation detectable by native-PAGE analysis (Fig 2E; compare to Fig 2A).

We concluded that pro-OmpA can acquire mis-folded intermediates that take it off-pathway for translocation, and these are no longer recognizable by TF.

TF:pro-OmpA complexes, but not TF, bind to the SecYEG-SecA translocase

We next sought to determine which stage of the pro-OmpA translocation reaction TF inhibits. To define whether inhibition lies prior to or post-translocase targeting, we preformed TF:pro-OmpA complexes in solution and quantified the subsequent delivery of pro-OmpA onto the SecYEG-SecA translocase. In this assay system, the binding of titrated concentrations of a [³⁵S]-labelled protein (as indicated) to SecA bound to SecYEG in IMVs is measured [9,10,61].

Both pro-OmpA and OmpA bind to SecYEG-bound SecA with high affinities when diluted from chaotrope straight into the SecYEG-SecA reaction [0.47 (\pm 0.07) and 0.65 (\pm 0.13) μM , respectively; Fig 3A, lane 2, top and middle]. In contrast, the off-pathway I₃ intermediate has no affinity for the translocase (Fig 3A, lane 2, bottom), in agreement with its lack of stimulation of the translocation ATPase of SecA (Figs 2D, lane 3; and EV4B).

As seen for other preproteins [61], neither pro-OmpA nor OmpA binds to SecYEG when SecA is absent (Fig 3A, lane 1). Like pro-PhoA [9,61], pro-OmpA docks to SecYEG-bound SecA bivalently. SecA(noSP), an alanyl substituted derivative that cannot bind SPs [62], still binds pro-OmpA and OmpA with the K_d of the mature domain (lane 3). Similarly, SecA(noPatchA), an alanyl substituted derivative of the mature domain binding site on SecA [9], cannot bind OmpA but still binds pro-OmpA (lane 4).

Trigger factor alone displayed no measurable binding to SecYEG-bound (Fig 3B, lane 2) or to soluble (Appendix Fig S4) SecA. In contrast, TF:pro-OmpA bound to SecYEG-SecA with a K_d of 1.79 (\pm 0.58) μM (Fig 3C). We obtained identical results with either TF: [³⁵S]-pro-OmpA (row 1) or [³⁵S]-TF:pro-OmpA (row 2), suggesting that TF remains complexed with pro-OmpA. This binding remains

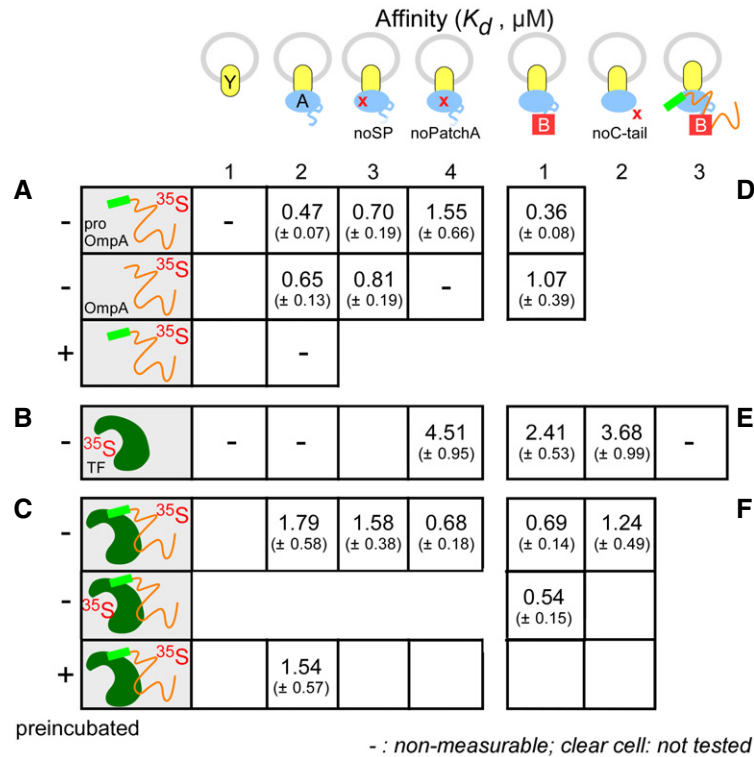


Figure 3. Equilibrium dissociation constants (K_d) of proteins and complexes for the Sec translocase.

A–F Equilibrium dissociation constants (K_d) of protein ligands (as indicated) for SecYEG-IMVs with or without SecA or its derivatives or SecB. Data analysed by non-linear regression and average values with standard mean error (SEM) are shown; $n = 6$ –9 biological replicates.

Source data are available online for this figure.

unaffected by a 10-min incubation of the TF:pro-OmpA complex at 37°C prior to its addition to SecYEG-SecA (Fig 3C). Thus, TF binding prevents formation of the translocation incompetent I_3 intermediate (compare to Fig 3A, bottom; preincubation of pro-OmpA alone). However, the affinities of pro-OmpA and of TF:pro-OmpA for the Sec translocase differ [$K_d = 0.47 (\pm 0.07)$ vs. $1.79 (\pm 0.58) \mu\text{M}$, respectively; Fig 3A and C]. We presume TF binding biases a different pro-OmpA “state” or shields binding sites, hence leading to a drop in the affinity for the SecA receptor. Mutations in the SP binding site of SecA did not alter the K_d of TF:pro-OmpA [$1.79 (\pm 0.58)$ vs. $1.58 (\pm 0.38) \mu\text{M}$; Fig 3C] although they did so for free pro-OmpA (Fig 3A), corroborating our hypothesis. TF-bound pro-OmpA may dock onto SecA using mainly PatchA, the mature domain binding site [9]. TF:pro-OmpA binds better to the SecYEG-bound SecA (noPatchA) than that to the wild-type translocase [$K_d = 0.68 (\pm 0.18)$ vs. $1.79 (\pm 0.58) \mu\text{M}$; Fig 3C] and better than the free pro-OmpA to the same mutant receptor [$K_d = 0.68 (\pm 0.18) \mu\text{M}$ (Fig 3C) vs. $1.55 (\pm 0.66) \mu\text{M}$ (Fig 3A)]. These observations support the possibility that pro-OmpA adopts an altered conformation upon TF binding or/and even that TF has its own independent contribution to SecA binding (see below).

We concluded that while TF does not bind to the SecA-SecYEG translocase with a measurable K_d , it accompanies the pro-OmpA client as it binds onto its SecA receptor and remains bound to it. Clearly, TF becomes deleterious for translocation at a post-targeting step.

SecB prevents pro-OmpA from acquiring off-pathway folding intermediates

SecB relieves the inhibitory effect of TF on pro-OmpA translocation (Fig 1D, lane 4). Given the data above, we entertained three hypotheses: (i) SecB may bind to pro-OmpA molecules released from TF, that we consider unlikely, taking into account the determined K_i (Fig 1E); (ii) SecB binding to soluble TF:pro-OmpA complexes releases pro-OmpA in solution allowing its independent self-targeting to the translocase; c. SecB binding at or near to translocase-docked TF:pro-OmpA complexes releases pro-OmpA for subsequent translocation.

We first examined whether SecB exerts an effect directly on pro-OmpA. For this, the ability of SecB to prevent formation of the I_3 intermediate was monitored by incubating $0.5 \mu\text{M}$ pro-OmpA with a range of SecB concentrations (0 – $2 \mu\text{M}$ SecB₄), at 37°C, for 10 min, prior to the SecYEG-SecA translocase addition and measuring the translocation ATPase of SecA. The effect of SecB on the T/M ratio was determined, normalized, plotted and analysed as in Fig 1F. SecB interacts with pro-OmpA directly, with a solubilization parameter K_{sol} of $190 (\pm 45)$ nM, prevents formation of the I_3 intermediate and leads to high translocation ATPase (Fig 4A). Moreover, in another functional assay similar to that in Fig 2C, SecB promotes the solubility of the aggregation-prone pro-OmpA* (Fig 4B).

However, in contrast to what was observed with TF:pro-OmpA (Fig 2A), SecB:pro-OmpA (Fig 4C) or SecB:pro-OmpA* (Appendix

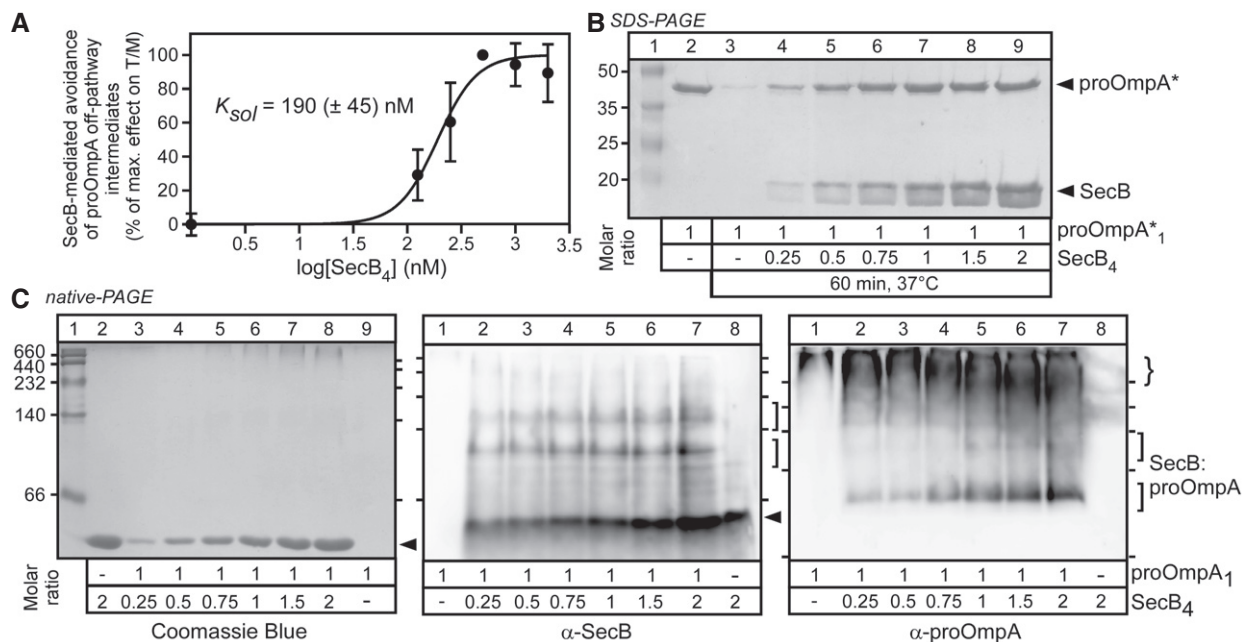


Figure 4. Physical and functional interaction of SecB with pro-OmpA and TF.

- A** SecB maintains soluble translocation-competent states of pro-OmpA at 37°C. pro-OmpA₁ (0.5 μ M) was incubated with a range of SecB₄ concentrations (0–2 μ M; Buffer D; < 0.2 M urea; 10 min, 37°C). Soluble samples (20,000 g; 10 min; 4°C) were added to translocation ATPase reactions (as in Fig 1C). Normalized T/M ratios were plotted ($n = 2$ –8 biological replicates; mean values \pm SEM) and an apparent solubilization constant (K_{sol}) determined (as in Fig 1F).
- B** SecB protects pro-OmpA* from aggregation. pro-OmpA*₁ (5 μ M) was incubated (50 μ l; Buffer C; 37°C; 60 min) alone or in the presence of the indicated molar excess of SecB₄, and pro-OmpA* in the soluble fraction (after centrifugation) was analysed by SDS-PAGE (as in Fig 2C). Lane 2: 2.84 μ g pro-OmpA*. Representative experiment is shown; $n = 4$ biological replicates.
- C** SecB physically interacts with pro-OmpA. pro-OmpA₁ (5 μ M) was incubated (50 μ l; Buffer C; < 0.2 M urea; 4°C; 60 min), with the indicated molar excess of SecB₄ (filled arrow), analysed by native-PAGE as in Fig 2A and stained as indicated. Brace: higher order pro-OmpA species. Representative experiment is shown; $n = 5$ biological replicates.

Source data are available online for this figure.

Fig S3) complexes could not be detected on Coomassie Blue-stained clear native-PAGE gels (Fig 4C, left). Immunostaining with α -SecB (middle) and α -pro-OmpA (right) antisera revealed two distinct but minor populations of SecB:pro-OmpA complexes (brackets), while most of pro-OmpA entered the gel and was detectable in high apparent masses (brace). A $K_{d,app}$ of 3 μ M was calculated (Appendix Fig S3), suggesting a high K_{off} and rapid dissociation. Native-MS detected SecB as a homotetrameric complex of 68764 ± 0.7 Da (Appendix Fig S5) that forms a 1:1 heterocomplex of $107,108 \pm 1.4$ Da with pro-OmpA.

Given the weaker K_d , \sim 15-fold less than that of TF for pro-OmpA (Fig 1E), it seems unlikely that the first hypothesis can adequately explain how SecB relieves TF-mediated inhibition with such fast kinetics.

Soluble TF:pro-OmpA:SecB quaternary super-complexes

We next examined whether SecB can associate with TF:pro-OmpA complexes in solution using four methods.

Firstly, we used native-MS and determined the association of the TF:pro-OmpA complex with the SecB apoprotein. TF:pro-OmpA associates with SecB to form a super-complex of 157,311 consistent only with a TF₁:pro-OmpA₁:SecB₄ stoichiometry (Figs 5A and B, and EV3).

Secondly, we used isothermal titration calorimetry (ITC). While SecB has no measurable affinity for TF (Appendix Fig S4B), titrating SecB₄ in preformed equimolar TF:pro-OmpA complexes revealed an affinity of $0.8 (\pm 0.18) \mu$ M and a stoichiometry of one SecB₄ per TF:pro-OmpA (Fig EV4A).

Thirdly, soluble TF:pro-OmpA:SecB complexes were observed by gel permeation chromatography coupled online to multiangle laser light scattering (GPC-MALS; Fig 5C). Upon mixing TF:pro-OmpA with SecB₄, a quantitative shift was observed to a higher mass peak, suggesting formation of a holo-complex that displayed some polydispersity. Ensemble measurements yielded a mean mass of \sim 137 (± 6) kDa; consistent with TF₁:pro-OmpA₁ bound to 2–4 SecB.

Fourthly, using native-PAGE (Fig EV4B) SecB₄ migrates with an apparent mass of \sim 50 kDa in this gel system, seen after Coomassie Blue staining (Fig EV4B, top, lane 3). When SecB is mixed together with TF:pro-OmpA (lane 7) a new, slower migrating species appears with higher apparent mass than that of TF:pro-OmpA (lane 6) and the intensity of the TF:pro-OmpA complex band is reduced. This presumed ternary TF:pro-OmpA:SecB super-complex is not detectable when SecB₄ is added to pro-OmpA (lane 5) or to TF₂ (lane 8) alone. The TF:pro-OmpA:SecB super-complex is immuno-stained using anti-sera to each of the three partner proteins (Fig EV4B, bottom panels).

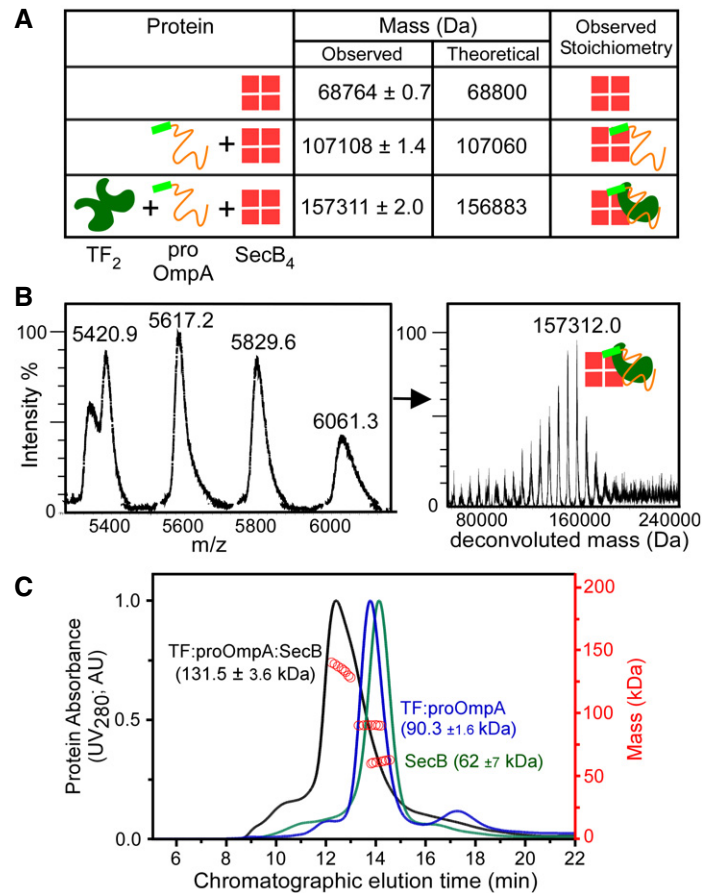


Figure 5. TF:pro-OmpA:SecB super-complex analysis.

A Analysis of pro-OmpA:SecB and TF:pro-OmpA:SecB complexes by native-MS. SecB₄ (30 μM; Buffer G), SecB₄ (40 μM) and pro-OmpA (20 μM; pre-treated with 10 mM DTT; buffer G) and of SecB₄ (40 μM), pro-OmpA (20 μM) and TF₂ (20 μM) in Buffer G were analysed as in Fig 2B (raw data in Fig EV3). *n* = 2 biological replicates.

B Blow up of the ESI-mass spectrum of the TF:pro-OmpA:SecB₄ super-complex from A (complete dataset in Fig EV3). Left: charge state distributions, at the indicated *m/z* range. Right: masses deconvoluted from the mass spectra (as in Fig 2B). Inset cartoon depicts stoichiometry. Representative spectrum is shown; *n* = 2 biological replicates.

C TF:pro-OmpA:SecB super-complex analysis using GPC-MALS in Buffer A. TF₁:pro-OmpA₁ (10 μM each; green), SecB₄ (40 μM; blue) and TF₁:pro-OmpA₁:SecB₄ (10, 10 and 40 μM, respectively; black). *n* = 5 biological replicates; mean mass: 137 kDa (± 6 kDa) representative experiment is shown; red circles: determined mass (kDa); AU: arbitrary units.

Source data are available online for this figure.

Taken together, these data demonstrate that SecB forms a previously unknown high-affinity quaternary complex with TF and pro-OmpA in solution *in vitro*, and therefore, likely in the cytoplasm. Formation of this stable complex suggests that SecB binding to TF:pro-OmpA is unlikely to promote significant pro-OmpA release.

SecYEG/SecA-bound SecB optimizes TF and TF:pro-OmpA binding to SecA

SecB does not affect pro-OmpA or OmpA affinity for the translocase significantly [0.47 (± 0.07) or 0.65 (± 0.13) μM (Fig 3A) vs. 0.36 (± 0.08) or 1.07 (± 0.39) μM (Fig 3D), respectively]. However, although TF shows no measurable affinity for the wild-type translocase (Fig 3B, lane 2), it acquired a substantial one in the presence of SecB [2.41 (± 0.53) μM; Fig 3E, lane 1]. Since the

direct binding of TF to SecB in solution is beyond detection (Fig EV4B, lanes 8; Appendix Fig S4), this suggested that somehow, SecB binding to the translocase might provide additional receptor sites or/and allosterically alters SecA, leading to TF binding. In support of this hypothesis SecB improved TF:pro-OmpA binding onto the wild-type translocase; 0.69 (± 0.14) (Fig 3F, lane 1) vs. 1.79 (± 0.58) μM (Fig 3C, top, lane 2). However, despite the presence of SecB, if pro-OmpA is already docked on SecA, TF no longer recognizes the wild-type translocase (Fig 3E, lane 3). We entertain two possibilities: the translocase binding sites for TF that SecB had exposed are hidden by pro-OmpA or a pro-OmpA-induced conformational change in the translocase makes these sites unavailable to TF binding [61].

SecB interacts with the SecA C-tail region, known to co-ordinate metal ions like Zn²⁺ [25,43,63]. Moreover, the C-tail residues 849–854 form a β-strand [9,62,64] that binds to PatchA, the mature

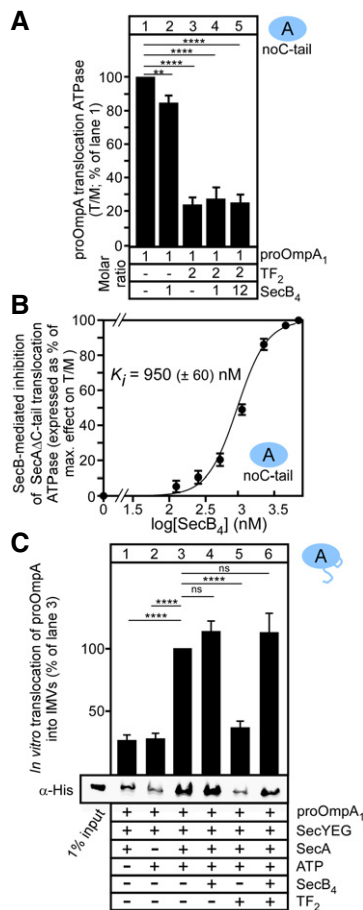


Figure 6. SecB-mediated, SecA C-tail-dependent release of TF-associated pro-OmpA for translocation.

A SecB fails to restore pro-OmpA translocation ATPase activity stimulation of SecA(noC-tail) in the presence of TF. pro-OmpA translocation ATPase activity stimulation (as in Fig 1C; SecB molar excess over pro-OmpA indicated). T/M ratio of SecA(noC-tail) in the absence of TF or SecB = 100%; lane 1; all other values were expressed as a % of this value. $n = 4$ biological replicates; mean values \pm SEM. Unpaired parametric t-test, 95% confidence interval: $***P = 0.0048$; $****P < 0.0001$.

B Excess of SecB inhibits the pro-OmpA-stimulated translocation ATPase activity of SecA(noC-tail). ATPase measured as in Fig 1C; SecB concentration range: 0–6 μM . Values were normalized (effect_{max} = 100%; effect_{min} = 0%) and plotted ($n = 3$ biological replicates; mean values \pm SEM) versus the $\log_{10}[\text{SecB}_4]$. The K_i was determined as in Fig 1E.

C TF and SecB-regulated, SecA-dependent *in vitro* translocation of pro-OmpA into SecYEG/A-IMVs, analysed after proteolytic treatment. Translocated, protease-resistant pro-OmpA was visualized using immunostaining (α -His) in the absence or presence of TF₂ or/and SecB₄ (as indicated). Translocation in the absence of TF or SecB was considered 100% (lane 3); all other values were expressed as a percentage of this. A summary of all repeats is presented (mean \pm SEM; $n = 6$ biological replicates; ns: not significant ($P = 0.1568$ for lane 3 vs. 4; $P = 0.4835$ for lane 3 vs. 6); Unpaired parametric t-test, 95% confidence interval: $****P < 0.0001$) with a representative Western blot (bottom).

Source data are available online for this figure.

domain binding site of SecA [9], thereby acting as a substrate mimic [62]. A SecA(noC-tail) derivative, missing the 70 C-terminal residues, is fully functional *in vivo* [65] and was shown to be

inhibited by TF in a genetic complementation assay (Appendix Fig S6A). We quantified the binding of TF to the SecA(noC-tail) (Fig 3E, lane 2). In the absence of SecB, TF exhibited an affinity for the SecYEG-bound SecA(noC-tail) [$3.68 (\pm 0.99) \mu\text{M}$] similar to the one seen in the presence of SecB for the wild-type translocase [$2.41 (\pm 0.53) \mu\text{M}$; lane 1]. Our inability to detect TF interaction with SecA(noC-tail) in solution (by ITC; Appendix Fig S4C) suggested that SecA(noC-tail) becomes primed for its interaction with TF by its prior binding to SecYEG.

Our results reveal a previously unsuspected TF:Sec translocase interaction that is conditional on a specific SecA conformation, induced by SecB binding. Attesting to this, SecA(noC-tail) undergoes measurable conformational changes, detectable by local HDX-MS (Fig EV5), that may underlie its conversion to a higher affinity TF receptor. This new unexpected role of SecB renders it an important determinant for the targeting of either TF or TF:pro-OmpA complexes to the translocase.

SecB requires the SecA C-tail to overcome the TF-mediated secretion inhibition

SecB exhibits high affinity for soluble [25] or membrane-bound (0.2–0.33 μM ; Fig EV1E; [44]) SecA and is released from it upon ATP hydrolysis [41]. Although SecB binding to SecA occurs in a C-tail-dependent manner [25,43,44,63], the C-tail of SecA *per se* is not essential *in vivo* or *in vitro* [65]. Corroborating this, pro-OmpA stimulated the translocation ATPase of SecA(noC-tail) (Fig 6A, lane 1) similarly to that of wild-type SecA (Fig 1C and D) [65]. SecB addition had no effect (Fig 6A, lane 2). TF suppressed this ATPase by 80% (lane 3), similarly to the effect seen on wild-type SecA (Fig 1D, lane 3). However, in contrast to what was seen for the wild-type SecA (Fig 1D, compare lanes 3 and 4), further addition of SecB, even up to 12 molar excess (Fig 6A, lane 5), did not relieve the TF-mediated inhibition (compare lanes 4 and 5 to 3).

Notably, even SecB when added to translocation ATPase reactions with SecA(noC-tail) becomes deleterious at high concentrations and inhibits pro-OmpA-stimulated translocation ATPase (Fig 5B). This presumably results from SecB exerting its holdase function on pro-OmpA but being unable to productively interact with the translocase in the absence of the SecA C-tail.

We concluded that productive SecB binding to the SecA C-tail is necessary to relieve the TF- or SecB-mediated inhibition of pro-OmpA translocation.

SecYEG/SecA-bound SecB acts as a preprotein- and TF-exchange factor

Our data demonstrated that the TF:pro-OmpA complexes arrive at and bind to the translocase (Fig 3C). Yet, pro-OmpA is probably not liberated from TF as indicated by the difference in the affinity of TF:pro-OmpA [$1.79 (\pm 0.58) \mu\text{M}$; Fig 3C] to that of free pro-OmpA [$0.47 (\pm 0.07) \mu\text{M}$; Fig 3A]. This affinity is restored when SecB is present [$0.69 (\pm 0.14) \mu\text{M}$; Fig 3F]. We hypothesized that SecB, that recognizes the TF:pro-OmpA complex even in solution [$0.8 (\pm 0.18) \mu\text{M}$; Fig EV4], can only somehow dissociate TF from pro-OmpA onto the translocase, thus allowing pro-OmpA translocation.

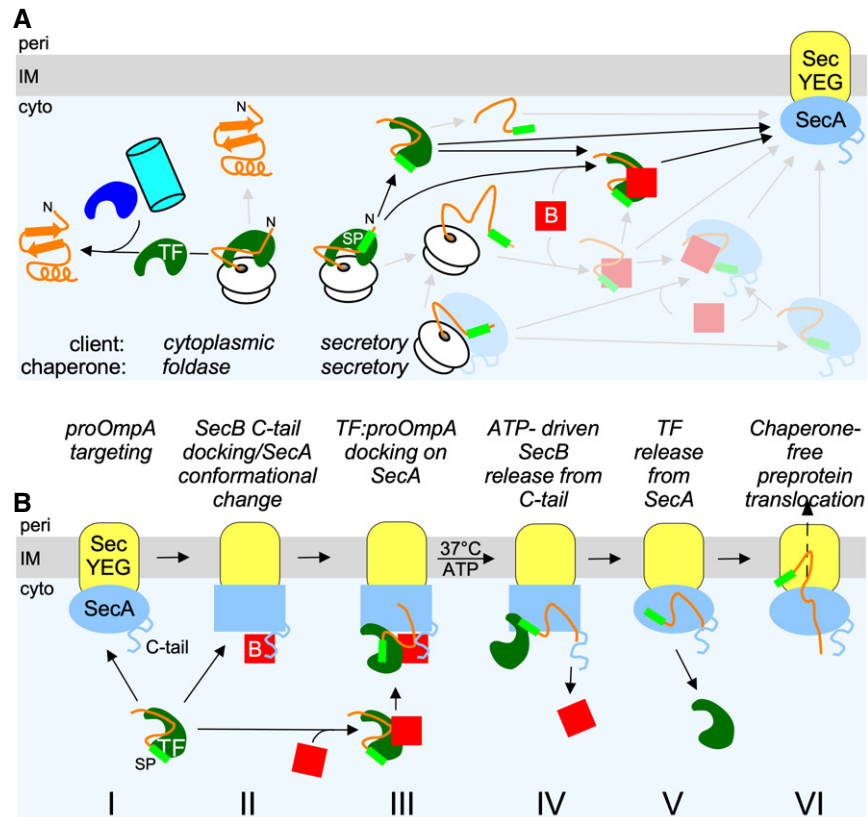


Figure 7. Models of TF involvement in the post-translational secretory pathway.

A Cartoon of the contribution of TF in cytoplasmic protein folding (left) and secretory protein targeting (right, black arrows). The secretory targeting factors SecB and SecA that act independently (grey arrows) or interface with TF are also shown. Blue, cyan: other folding chaperones.

B Schematic model of TF:pro-OmpA targeted to the translocase with or without contributions from SecB and subsequent SecA C-tail/SecB-mediated control of pro-OmpA translocation. Oval to rectangle transition in SecA signifies conformational changes. B: SecB; cyto: cytoplasm; IM: inner membrane; peri: periplasm.

We directly tested this hypothesis by using an *in vitro* pro-OmpA translocation assay [9]. pro-OmpA is translocated into the lumen of IMVs and thus becomes protease-resistant, in a SecA and ATP-dependent manner (Fig 6C, lanes 1–3). SecB seems to slightly increase pro-OmpA translocation (lane 4). Addition of TF alone inhibits (lane 5), but further addition of SecB restores (lane 6) pro-OmpA translocation. Similar results were obtained with [³⁵S]-pro-OmpA synthesized in the absence of urea, thus excluding a chaotrope-related artefact (Appendix Fig S6B).

We concluded that SecB bound at the SecYEG-SecA translocase acts as an exchange factor, causing pro-OmpA release from TF to permit its translocation.

Discussion

Trigger factor is one of the ~200 universally conserved proteins in the bacteria [27,66,67] and has a well-understood role in cytoplasmic protein folding [27] (Fig 7A, left), but its precise role in post-translational secretion (Fig 7A, right) has remained unclear. A perplexing observation has been that TF retards protein export *in vivo*, since *tig* mutations increased the Sec-dependent export of some clients [22,50,68]. When overexpressed, TF actually

compromises translocation *in vivo* [50] and viability [22]. As SecB relieves this deleterious effect [22], it was anticipated that overexpressed TF may specifically block a secretion pathway step possibly through its ribosome-associating capacity: ribosome-bound TF sterically hinders the association of ribosomes with the SecYEG translocase [22].

We now show that TF is a *bona fide* secretory pathway chaperone as follows: (i) it forms tight complexes with a subset of secretory preproteins such as pro-OmpA, co- [69] and post-translationally (Figs 1E and 2A; [29]) and can prevent their aggregation (Fig 2C; [28,39]) or acquisition of off-pathway folding intermediates (Figs 2D and 3C, and EV2); (ii) when complexed to pro-OmpA it binds to SecB in solution (Figs 5B and C, EV3 and EV4A and B) and to SecYEG-bound SecA with high affinity (Fig 3C); (iii) in the presence of SecB, but not in its absence, TF binds to SecYEG-bound SecA with high affinity even in the absence of pro-OmpA (Fig 3E); and d. TF does not allow pro-OmpA, that is co-targeted to the translocase, to proceed to translocation (Figs 1D and 6A and B) unless it is first recycled by SecB acting via the SecA C-tail (Figs 1D and 6A and B). Reconstitution of the TF-mediated inhibition reaction *in vitro* and use of the non-ribosome binding 3A mutant (Fig 1A, lane 8) revealed that the role of TF is largely ribosome-independent and hence post-translational. This intricate and

remarkable network of interactions in which TF physically participates was previously unsuspected and extends the functional interactome of TF to the Sec translocase. The association of TF with the membrane may explain, at least partly, why in proteomics experiments TF is systematically identified in the inner membrane periphery [70].

That TF specializes on only a limited set of secretory clients might explain its non-essentiality for protein secretion. Of the 108 secretory chains that TF recognizes on ribosomes [6,69], only 10 are found to be TF-associated after synthesis [6]. A second reason is that targeting in the secretion pathway has in-built redundancy (Fig 7A, right), as does the folding pathway (Fig 7A, left) [48]. For example, as an alternative to using TF, pro-OmpA might be briefly complexed with SecB (Fig 4A–C; [44,71]) or SecA [72] or a complex of both [44,72]. The intracellular concentrations of TF, SecB, SecA and their affinities for each other and for pro-OmpA (Figs 3 and EV1, and EV4A) will direct/orchestrate these interactions “on demand” *in vivo*. Since all three chaperones can make use of either the SP or the multiple mature domain stretches of a preprotein [9,16,42], even multiple different chaperones may assemble on the same preprotein, as proposed for TF and DnaK [73], or for multiple TFs interacting with the same unfolded secretory polypeptide [16].

Trigger factor does not display a generic preference for slightly hydrophobic outer membrane porin β -barrels although it interacts strongly with some of them. It associates with ~25% of all nascent outer membrane proteins that constitute < 3% of all its nascent interactors [6,69], co- or post-translationally (e.g. OmpX; Appendix Fig S3) [6,74]. Therefore, it is unclear why TF would specialize on pro-OmpA as a client. It may recognize particular structural features on pro-OmpA. Alternatively, such specialization may have derived from pro-OmpA's disposition to acquire “off-translocation pathway” intermediates (Figs 2E and EV2) and/or the fact that pro-OmpA is one of the most abundant cellular proteins (~100,000 to ~150,000 copies/cell [1]). Any disruption or slow down of secretion flow will result in the accumulation of large amounts of cytoplasmic pro-OmpA. TF may sequester these molecules queuing for translocation to prevent their mis-folding or aggregation and ensure their delivery to the translocase, once sufficient amounts of SecB/SecA become available. This hypothesis is in line with the fact that non-stressed cells do not need TF to accomplish pro-OmpA secretion since there is no perturbation of the secretion flow and hence no accumulation of pro-OmpA molecules [40].

Secretory protein recognition and targeting by TF must be governed by some specificity to avoid futile interactions: e.g. neither TF:pro-OmpA should be passed on to cytoplasmic foldases, nor TF:cytoplasmic clients should reach and stochastically interfere with the operation of the translocase. Kinetic “bottlenecks” may render such “illicit” interactions less likely, such as short TF:client lifetimes or, downstream chaperones at high concentrations and/or elevated affinities for TF:clients. Correct vectorial transfer to the right pathway, cytoplasmic or secretory, may be additionally secured by SPs for a fraction of exported proteins. SPs may act as high affinity, secretion pathway-only handles, for tighter interactions with TF and subsequently with SecB and/or SecA (Fig 7A, right). For example, SecB binding to TF:pro-OmpA, with an increased affinity (Fig EV4A), will bias TF:pro-OmpA to stay on the secretory pathway and reach the translocase. In contrast, SecA may chaperone

cytoplasmic proteins for folding, thus additionally diverting them from the secretion pathway [75].

Non-ATPase chaperones, such as TF and SecB, are assumed to behave like typical holdases [16], i.e. will bind tightly, with long lifetimes, to a secretory polypeptide chain and prevent it from acquiring a folded state or aggregating. As most secretory proteins, including pro-OmpA, can maintain soluble non-folded or partially folded states in solution for long and are frequently disordered [11], this is not often/frequently necessary. However, if the need arises, TF residing at the ribosomal exit tunnel, its cytoplasmic concentration and high affinity for clients can secure a rapid interaction with secretory clients, preventing not only aggregation but also off-pathway folding intermediates (Figs 1E and 2A and C, and EV4B).

Of note, complexes of pro-OmpA with SecB, considered as the typical pro-OmpA chaperone [54], can be stabilized under certain conditions (Figs 4 and 6B; Appendix Fig S5) [76,77], were weaker than those of TF (Figs 1F and 4C; Appendix Fig S3D). Nevertheless, SecB rescued pro-OmpA from both mis-folding (Fig 4A) and aggregation (Fig 4B) [55]. The apparent high K_{off} of this interaction goes against the typical holdase concept. Perhaps even fleeting interactions with SecB return pro-OmpA to soluble states, reminiscent of binding/release cycles that clients undergo on foldase chaperones [78,79], while at elevated concentrations, the SecB holdase is stabilized (Fig 6B).

TF:secretory client complexes, with or without SecB, are specifically targeted to SecYEG-bound SecA (Fig 3). In this previously unsuspected reaction, TF:secretory client complexes bind to the translocase through the independent affinities of the secretory chain, TF and SecB for SecA and for each other. One remarkable aspect of this process extends the role of SecB beyond that of a typical chaperone. SecB bound via the SecA C-tail acts as a recycling regulator for TF:pro-OmpA complexes, overcoming the TF-mediated inhibition of pro-OmpA translocation (Fig 6A and C). The precise mechanistic, structural and dynamic basis of this process requires future dissection. Nevertheless, a key event in the process seems to be the conformational dynamics of the SecA motor, the only ATP hydrolysing enzyme in the dynamic holo-complex and, evidently, anticipated to be the core ATP-driven partner recycling component. Local HDX-MS (Fig EV5) and single molecule-FRET analysis [80,81] (S. Krishnamurthy, N. Eleftheriadis, K. Karathanou, S. Smit, A.G. Portaliou, K.E. Chatzi, M.F. Sardis, S. Karamanou, A. Bondar, G. Gouridis & A. Economou, in preparation) revealed such conformational events in various parts of the SecA structure including its preprotein binding domain. The enhanced affinity for TF of the two SecA derivatives, SecA(noPatchA) and SecA(noC-tail) (Fig 3B and E), raises the possibility that these two elements that are juxtaposed in the SecA structure, one binding mature domains (PatchA) and the other SecB (C-tail), may be central switches that modulate SecA conformation (Fig EV5) and, consequently, the affinity for TF.

Taken together, these and past data led to a simple working hypothesis for the translocation of secretory proteins co-targeted to the translocase with TF (Fig 7B). TF:pro-OmpA complexes are targeted to the translocase and bind to SecA with (II, III) or without (I) SecB. In the former case, binding is ~3 times tighter and could be attributed to SecB providing binding surfaces directly to TF and/or preprotein and to SecB-driven conformational changes onto SecA mediated through SecB occupancy of the SecA C-tail (III). Initiation of the translocation ATPase cycle expels SecB (IV) [43], and SecA

conformation is altered to a state that promotes dissociation of the TF:pro-OmpA complex. pro-OmpA is released from TF and binds with high affinity to SecA in a way that is no longer available for TF binding (Fig 3E). As a result of a reduced affinity for the SecA receptor, TF is expelled to the cytoplasmic pool (Fig 7B, V). SecA-bound pro-OmpA proceeds with translocation (VI).

Materials and Methods

For a complete list of strains (Appendix Table S1), plasmids (Appendix Table S2), primers (Appendix Table S3), buffers (Appendix Table S4), see Appendix.

In vivo genetic complementation assay

Wild-type MC4100, MC4100 Δ secB, MC4100 Δ tig Δ secB and BL21-19 cells transformed with plasmids carrying, or not, secA or secA Δ Ctail, tig or secB were grown overnight at 30°C in LB supplemented with ampicillin (100 μ g/ml) and gentamicin (10 μ g/ml) if needed. Cultures were diluted (1/50) into fresh LB and grown at 30°C until OD₆₀₀ = 0.5. Serial dilutions were spotted on freshly prepared LB plates containing antibiotics without or with anhydrotetracycline (AHT; 5 ng/ml) and without or with L-arabinose (0.1% w/v).

Chaperone-mediated solubilization assay using SDS-PAGE

Chaperones (in Buffer A) and pro-OmpA* (in Buffer B; without DTT/EDTA treatment) were mixed together at different molar ratios in Buffer C, incubated (37°C; 60 min) and centrifuged (20,000 g; 4°C; 10 min; Sigma 1-16K). Soluble proteins were analysed on a 15% acrylamide SDS-PAGE gel and Coomassie Blue stained. pro-OmpA signals were quantified by scanning densitometry (Image J; <https://imagej.net/Welch>).

Chaperone-pro-OmpA binding assay using native-PAGE

Chaperones (Buffer A) and pro-OmpA (Buffer B; DTT- and EDTA-treated) were mixed together at different molar ratios in aqueous Buffer C, or Das indicated, incubated (37°C; 60 min) and centrifuged (20,000 g; 4°C; 10 min; Sigma 1-16K). Soluble proteins were separated on a 10% acrylamide native-PAGE gel (4 mA; 4°C; 16 h) and Coomassie Blue stained.

Cell growth, gene overexpression and cell lysis

Escherichia coli Lemo21, BL21.19 or Tuner cells transformed with plasmids expressing preproteins, mature domains or chaperones (see "Plasmids" table S2 in Appendix), or BL31(DE3) cells, transformed with pET610 (carrying the his-secYEG operon), were grown in LB (37°C; 100 mg/ml Ampicillin; till OD₆₀₀ = 0.6), and gene expression was induced (0.1 mM IPTG; 3 h; 30°C) [11]. For preproteins, 4 mM sodium azide was added in the cell culture, 10 min prior to IPTG induction to prevent SecA-dependent secretion and thus SP cleavage [82]. Cells were harvested (5,000 g; 4°C; 15 min; Avanti J-26S XPI, JLA 8.1000 rotor; Beckman) and resuspended in Buffer I (preproteins, mature domains) or Buffer J (His-TF) or Buffer K (SecB) or Buffer L (SecA and derivatives) or Buffer M (SecYEG-IMVs). Cells were lysed using a French press (8,000 psi; 3–5 passes; pre-cooled cylinder at

4°C; Thermo). Unbroken cells were removed (3,000 g; 10 min; Sigma 3-16KL; rotor 11180), and supernatants were centrifuged further (35,000 g; 30 min; 4°C; Optima XPN-80, Beckman) to separate soluble from membrane proteins or/and inclusion bodies.

Protein purification

Denaturing protein purification of His-tagged proteins

The pellet of lysed cells was solubilized in Buffer N (Dounce homogenizing) and centrifuged (35,000 g; 30 min; Optima XPN-80; 45 Ti fixed-angle rotor; Beckman) [9,11]. The urea-solubilized supernatant was diluted with Buffer O to 6 M urea before applying it on a column packed with Ni²⁺-NTA agarose resin (1 ml/5 μ g protein; Qiagen) pre-equilibrated with Buffer P (gravity flow; 1 ml/min). The column was washed sequentially with Buffer P and Buffer Q (10 column volumes). Proteins were eluted with Buffer R, incubated with EDTA (10 mM; 30 min; 4°C), dialysed (12–14,000 Da molecular weight cut-off, Mediatech Membranes Ltd.; Buffer S; 12 h; 4°C), aliquoted and stored at –20°C. All purification and dialysis buffers were supplemented with 5 mM and 2.5 mM MgCl₂, respectively, to prevent SP cleavage [83].

Non-denaturing purification of His-tagged proteins

The supernatant of lysed cells was loaded on a column packed with Ni²⁺-NTA Agarose resin (1/ml resin/10 μ g of protein; Qiagen), pre-equilibrated with Buffer T (gravity flow; 1 ml/min) and washed with Buffer U [9,11]. Proteins were eluted with Buffer V, incubated with EDTA (10 mM; 30 min, 4°C) and dialysed first in Buffer W (3 h; 4°C) and then in Buffer X (12 h; 4°C). Proteins were aliquoted and stored at –20°C.

Purification of untagged SecB

The soluble supernatant was loaded on a column packed with a Q resin (5 ml; flow rate 1 ml/min; GE Healthcare) washed sequentially with 10 column volumes of Buffer Y, Buffer Z and Buffer AA [9–11]. SecB was eluted with Buffer AB and further purified using preparative gel permeation chromatography (HiLoad Superdex 200; Buffer AC; ÄKTA Pure System; GE Healthcare). Peak fractions (5 ml) were collected, pooled and dialysed: Buffer W (12 h; 4°C) then in Buffer X (12 h; 4°C). Protein aliquots were stored at –20°C.

Purification of untagged SecA and derivatives

Following cell lysis, the soluble supernatant was loaded (2 ml/min) on a pre-equilibrated home-prepared Cibacron Blue resin (Sigma) [9–11]. The column was washed (Buffer AD; 10 column volumes; 2 ml/min; ÄKTA Pure System; GE Healthcare), and SecA was eluted using a linear gradient (Buffer AD to Buffer AE; 4 column volumes; 2 ml/min), in 5 ml fractions, and concentrated, and NaCl was adjusted to 1 M final concentration. Following DTT treatment (20 mM; 15 min; 4°C), SecA was loaded on a preparative HiLoad Superdex 200 (GE Healthcare) gel permeation chromatography column (Buffer AC). Peak fractions (5 ml) were collected, concentrated, treated with 10 mM DTT and re-loaded on a second HiLoad Superdex 200 (GE Healthcare) pre-equilibrated with Buffer A. Fractions containing SecA were pooled and dialysed in Buffer X (12 h; 4°C). Protein aliquots were stored at –20°C.

Determination of protein concentration

Protein concentrations were determined spectroscopically (280 nm; NanoDrop 2000; Thermo) [9,11]. The molecular weight and

extinction coefficient of proteins were determined using the ExPasy server (<http://web.expasy.org/protparam/>). Spectroscopic measurements were also employed to determine the soluble/aggregation character of proteins alone (Fig EV3B). The initial protein concentration (the input = 100%, at 0 min) was compared to protein concentration in the supernatants after centrifugation (20,000 g; 4°C; 10 min; Sigma 1-16K) after an incubation (time and temperature as indicated). Wherever indicated, pre-treatment of protein stock solutions was with 10 mM DTT, 5 mM EDTA (20 min; 4°C).

Preparation of inverted inner membrane vesicles (IMVs)

Following lysis by French press and removal of unbroken cells (4,000 g; 10 min; Sigma 3-16KL; rotor 11180), samples were ultracentrifuged (95,000 g; 90 min; 4°C; 45 Ti fixed-angle rotor; Optima XPN-80, Beckman) [9,11]. The membrane pellet was resuspended (2 ml; Buffer AF; Dounce-homogenizer), loaded on top of a 5-step sucrose gradient (1.9; 1.7; 1.5; 1.3; 1.1 M sucrose in Buffer AF; 6 ml each layer) and centrifuged to equilibrium (84,000 g; 16 h, 4°C; SW 32 Ti swinging bucket rotor, Optima XPN-80, Beckman). IMVs, collected from gradient fraction 2, were resuspended (Buffer AG) and re-centrifuged (95,000 g; 90 min; 4°C; fixed-angle T647.5 rotor, Sorvall). The membrane pellet was resuspended and Dounce-homogenized in Buffer AH (20 min; 4°C), loaded on top of an equal volume of Buffer AI and centrifuged (95,000 g; 90 min; 4°C; T647.5 rotor; Beckman). IMVs were collected [84], Dounce-homogenized in 2 ml of Buffer D and extruded through a 100-nm pore size filter (15–21 passes; Avestin LiposoFast-Basic system), to obtain unilamellar vesicles of similar diameter, and stored in aliquots at –80°C.

Measuring SecA ATPase activity

ATP hydrolysis was measured in Buffer E (50 µl) [85–87]. To determine basal ATPase activity, 0.4 µM SecA was added; for membrane ATPase, SecYEG-IMVs were added (0.4 µM SecY; for membrane/basal ratio 1.4; [85]); and for translocation ATPase, preprotein (as indicated) was added. SecB and TF were added (as indicated). In the case preincubation is indicated, the preprotein (–/+ chaperone) was incubated (Buffer D; 40 µl; 10 min; indicated temperature) and centrifuged (20,000 g; 10 min; 4°C) and the supernatant was added to SecA-SecYEG (as for translocation ATPase setup). After incubation at 37°C (20 min for basal and membrane; 10 min for translocation), the released inorganic phosphate (Pi) was measured using malachite green reagent and the K_{cat} (pmol Pi/pmol SecA protomer/min) was determined.

[³⁵S]-labelling of proteins *in vitro*

Proteins were labelled with [³⁵S]-methionine (1,000 Ci/mMole; Perkin-Elmer) during *in vitro* synthesis, using a TNT Quick coupled Transcription/Translation system (Promega) according to the manufacturer's instructions [9,11]. [³⁵S]-labelled proteins were separated from the free unincorporated radiolabelled amino acids by centrifugal filtration (1-ml homemade insulin syringe columns; packed with G-50 resin; pre-equilibrated with Buffer F for TF and SecB or Buffer AJ for pro-OmpA; centrifuged for 5 min (4°C; 3,000 g; Sigma 3-16KL; rotor 11180). Flow-through was further centrifuged to

remove ribosomes (436,000 g; 20 min; 4°C; rotor TL-100; Optima Max-XP, Beckman-Coulter) and stored at –20°C. For *in vitro* translation/translocation reactions, following synthesis of [³⁵S]-pro-OmpA and removal of ribosomes, protein in Buffer F was immediately used for translocation reactions (see below).

Determination of equilibrium dissociation constants (K_d) for SecYEG-bound SecA

SecA (0.4 µM) mixed with SecYEG-IMVs (0.4 µM SecY) and SecB (1 µM; whenever indicated) was pre-incubated (4°C; 10 min; in 10 µl of Buffer F) [9,11,61]. Pre-treated pro-OmpA or OmpA stocks (10 mM DTT; 20 min; 4°C; then centrifuged at 20,000 g; 20 min; 4°C) were diluted in Buffer F in order to achieve a range of 0–2.4 µM in 200 µl. For TF, a range of 0–24 µM was used and for SecB 0–1 µM. Where indicated, pro-OmpA or TF:pro-OmpA dilutions were pre-incubated (10 min; 37°C) prior to addition to the binding reactions. Proteins were added to SecA-SecYEG(-SecB) binding reactions (final 0–0.6 µM range for SecB, OmpA, pro-OmpA; 0–6 µM for TF). 2 µl of [³⁵S]-protein was added to all samples as a tracer. Samples were incubated (20 min; 4°C), overlaid on an equal volume of BSA/Sucrose cushion (Buffer AK) and centrifuged (436,000 g; 20 min; 4°C; rotor TL-100; Optima Max-XP, Beckman-Coulter). The pellet (containing IMVs and IMV-bound proteins) was resuspended (300 µl Buffer F), and samples were immobilized on a nitrocellulose membrane (Protran, 0.4 mm) using a vacuum manifold (Bio-Dot apparatus; Bio-Rad). Bound [³⁵S]-labelled proteins on IMVs were visualized using a high-resolution phosphor storage screen (GE Healthcare) on a Typhoon FLA 9500 system (GE Healthcare; default system settings) and quantified by Image Quant software (GE Healthcare). Data were analysed by non-linear regression (one binding site fit; GraphPad Prism 6). For the determination of each K_d , $n = 6$; 20 concentration points were used. Binding of proteins to the SecYEG-IMVs in the absence of SecA showed only non-saturable binding assumed to be on lipids.

pro-OmpA *in vitro* translocation

pro-OmpA (Buffer AJ or F) was pre-treated (10 mM DTT; 5 mM EDTA; 20 min; 4°C) and centrifuged (20,000 g; 10 min; 4°C) [9]. Translocation reactions (100 µl; Buffer F) with SecA (0.8 µM), SecYEG-IMVs (0.8 µM SecY), pro-OmpA (3 µM), TF₂ (3 µM), SecB₄ (3 µM) and ATP (2 mM) were incubated (30 min; 37°C) and transferred on ice. Non-translocated molecules were digested by addition of 1 mg/ml proteinase K (Roche; 20 min; 4°C). Proteins were precipitated with 25% w/v TCA (60 min; 4°C), analysed by SDS-PAGE (12% gels) and visualized by immunostaining with α-His antisera (Serotec) using α-mouse horseradish peroxidase-coupled secondary antibody (Jackson ImmunoResearch Laboratories, Inc.). Signals were visualized using the Supersignal West Pico kit (Thermo Fisher Scientific) in a CCD-camera system (LAS-4000; GE Healthcare) and quantified using Image J (<https://imagej.net>).

Native-mass spectrometry (Native-MS)

Trigger factor was exchanged in Buffer G (overnight; 4°C). pro-OmpA was diluted in the dialysed TF in a 1:1 molar ratio and incubated (10 min) before it was subjected to mass spectrometric

analysis. 30 μM of the sample was injected for native-mass analysis using electrospray ionization mass spectrometer with a Q-TOF mass analyser (Synapt G2 HDMS, Waters); sodium iodide (2 mg/ml) was used as a calibrant. The operating parameters for the spectral acquisition were as follows: capillary voltage, 1.8 kV; sample cone voltage, 60 V; extraction cone voltage, 2 V; source temperature, 37°C; desolvation temperature, 150°C; backing pressure, 5.9 mbar; source pressure, 2.08 e-3 mbar; and Trap, 1.44 e-3 mbar. Spectra were acquired in the range of 900–13,000 m/z in positive ion V-mode. The molecular mass of the recorded spectra was calculated using MassLynx software (MassLynx version 4.1) by deconvoluting the mass spectra using MaxEnt 1.

Global and local hydrogen–deuterium exchange-mass spectrometry (HDX-MS)

Protein folding experiments

pro-OmpA (Buffer AL) was pre-treated (10 mM DTT; 5 mM EDTA; 20 min; 4°C) and centrifuged (20,000 g; 10 min; 4°C) [11]. Folding was initiated by diluting pro-OmpA to 0.2 M urea with pre-warmed/chilled Buffer AM, at the indicated temperature and monitored up to 1 h ($t_{\text{fold}} = 1$ min, 5 min, 10 min, 15 min and 1 h).

Global pulsed HDX-MS

Lyophilized Buffer AM was freshly reconstituted in D_2O (99.9% atom D, Sigma-Aldrich 151882). At the indicated t_{fold} , samples containing 0.85 μM pro-OmpA were isotope labelled in 95.5% (v/v) D_2O (pD:8.0; 100 s; indicated temperature). Non-deuterated (ND) samples were prepared similarly, using protiated Buffer AM. Fully deuterated (FD) controls were labelled in Buffer AN (pD:8.0; 4°C; 1 h). All samples were quenched with pre-chilled formic acid (ice; final pD = 2.5), snap-frozen in liquid nitrogen and stored at -80°C until MS analysis (max 2 days; nanoACQUITY UPLC System with HDX technology—Synapt G2 ESI-Q-TOF; Waters). The UPLC sample chamber temperature was set at 0.2°C. pro-OmpA (42.6 pmol) was desalted [250 $\mu\text{l}/\text{min}$, 2 min; MassPREP Micro Desalting Column (Waters); 0.23% (v/v) formic acid] and eluted [40 $\mu\text{l}/\text{min}$; 5%–90% linear gradient of 0.23% (v/v) formic acid in acetonitrile]. Spectra were acquired in the 400–2,000 m/z range (capillary voltage, 3.0 kV; sampling cone, 40 V; extraction cone, 3.6 V; source temperature, 80°C; and desolvation gas flow, 500 L/h at 150°C). Continuous calibration was achieved by co-infusing Leucine Enkephalin (2 ng/ μl in 50% acetonitrile–0.1% formic acid; 5 $\mu\text{l}/\text{min}$; Waters).

Local HDX-MS

SecA and SecA (noC-tail) were prepared in 100 μM stock concentrations. The deuterium exchange reaction was initiated by diluting 200 pmol of protein into D_2O Buffer AO at a 1:10 ratio (final D_2O concentration 90%). Continuous deuterium labelling was carried out for various timepoints (10 s, 30 s, 1 min, 2 min, 5 min, 10 min, 30 min and 2 days) prior to quenching with pre-chilled quench solution (formic acid, 4 mM TCEP, 1 mg/ml fungal protease XII). The exchange reaction was mixed with quench solution at a 1:1 ratio to obtain a final pH of 2.5, and the reaction was incubated (2 min; 4°C). 100 pmol of SecA was injected into a nanoACQUITY UPLC System with HDX technology (Waters, UK) coupled to a SYNAPT G2 ESI-Q-TOF mass spectrometer. For enhanced peptide coverage, SecA was digested in 2 steps, first with fungal protease

XIII [88] at the quench step, and subsequently digested online on a home packed immobilized pepsin (Sigma) cartridge (2 mm \times 2 cm, Idex), at 16°C. HPLC and MS parameters were set as previously described [10]. Peptide identification was carried out using the ProteinLynx Global server (Waters, UK). Deuterium exchange data were analysed using DynamX (Waters, UK) [10,60].

Gel permeation coupled online to multiangle laser light scattering (GPC-MALLS)

Multiangle light scattering experiments were performed online after gel-permeation chromatography on a Superdex HR200 10/300GL mounted on an HPLC system (Optilab T-rex; Wyatt) coupled to a photodiode array detector (SPD-M10AVP; Shimadzu), a multiangle light scattering detector (DAWN-EOS; Wyatt) and a refractive index detector (RID10A; Shimadzu) [9,85]. TF₁:pro-OmpA₁ (10 μM each) and/or SecB₄ (40 μM) were loaded using a 100 μl injection loop, in Buffer A, and chromatographed at 22°C at 0.8 ml/min. Data collection, analysis and plotting were performed using Astra v.5.0 software (Wyatt).

Isothermal titration calorimetry (ITC)

TF:pro-OmpA and SecB samples were extensively dialysed (Buffer H) [61]. All solutions were filtered (0.45 μm) and thoroughly degassed (20 min; gentle stirring under vacuum). The cell was filled with TF₂:pro-OmpA₁ (15 μM ; 300 μl) and the syringe with protein ligands as indicated (128 μM ; 100 μl). For the titration, 2 μl injections, at 4-min intervals (cell temperature 25°C, constant stirring at 300 rpm), were used. The experiments were performed using a MicroCal iTC200 System (GE Healthcare). Data were analysed with MicroCal Origin software version 7.0 (GE Healthcare).

Data availability

All raw data used for figures and expanded view figures are provided as source data files.

Expanded View for this article is available online.

Acknowledgements

This paper is dedicated to the memory of Prof. Olaf Schneewind. We are grateful to P. Genevaux for strains; K. Chatzi, N. Famelis and L. Emmanouilidis for preliminary observations; and A. Tsirigotaki and N. Eleftheriadis for suggestions and biochemicals. Research in our lab was funded by grants (to AE): RiMemBR (Vlaanderen Onderzoeksprojecten; #G0C6814N; FWO); MeNaGe (RUN #RUN/16/001; KU Leuven); CARBS (#G093519N; FWO); ProFlow (FWO/F.R.S.- FNRS “Excellence of Science—EOS” programme grant #30550343) and (to AE and SK): FOscil (ZKD4582—C16/18/008; KU Leuven). JDG was an FWO doctoral fellow (#1553916N; FWO); SKr was an FWO [PEGASUS]² Marie Skłodowska-Curie Fellow (#12Q1417N; FWO).

Author contributions

JDG, AGP, BS, SKa and SKr purified proteins. JDG performed solubility, native-PAGE, ATPase and *in vivo* experiments. AGP performed molecular cloning, native-PAGE, membrane affinity, *in vitro* translocation and ATPase, TF expression, *in vivo* growth and GPC-MALLS experiments. BS performed ITC, native-MS experiments and *in vivo* experiments. SKr performed local HDX-MS. SKa

supervised and helped with biochemical and biophysical assays and data analysis and performed global HDX-MS experiments. AE, JDC, AGP and SKa wrote and revised the paper with contributions from BS. SKa and AE conceived and managed the project. All authors reviewed the manuscript.

Conflict of interest

The authors declare that they have no conflict of interest.

References

1. Tsirigotaki A, De Geyter J, Sostaric N, Economou A, Karamanou S (2017) Protein export through the bacterial Sec pathway. *Nat Rev Microbiol* 15: 21–36
2. De Geyter J, Tsirigotaki A, Orfanoudaki G, Zorzini V, Economou A, Karamanou S (2016) Protein folding in the cell envelope of *Escherichia coli*. *Nat Microbiol* 1: 16107
3. Rapoport TA, Jungnickel B, Kutay U (1996) Protein transport across the eukaryotic endoplasmic reticulum and bacterial inner membranes. *Annu Rev Biochem* 65: 271–303
4. Cross BC, Sinning I, Luirink J, High S (2009) Delivering proteins for export from the cytosol. *Nat Rev Mol Cell Biol* 10: 255–264
5. Smets D, Loos MS, Karamanou S, Economou A (2019) Protein transport across the bacterial plasma membrane by the sec pathway. *Protein J* 38: 262–273
6. Loos MS, Ramakrishnan R, Vranken W, Tsirigotaki A, Tsare EP, Zorzini V, Geyter J, Yuan B, Tsamardinos I, Klappa M et al (2019) Structural basis of the subcellular topology landscape of *Escherichia coli*. *Front Microbiol* 10: 1670
7. Veenendaal AK, van der Does C, Driessen AJ (2004) The protein-conducting channel SecYEG. *Biochim Biophys Acta* 1694: 81–95
8. Vrontou E, Economou A (2004) Structure and function of SecA, the preprotein translocase nanomotor. *Biochim Biophys Acta* 1694: 67–80
9. Chatzi KE, Sardis MF, Tsirigotaki A, Koukaki M, Sostaric N, Konijnenberg A, Sobott F, Kalodimos CG, Karamanou S, Economou A (2017) Preprotein mature domains contain translocase targeting signals that are essential for secretion. *J Cell Biol* 216: 1357–1369
10. Sardis MF, Tsirigotaki A, Chatzi KE, Portaliou AG, Gouridis G, Karamanou S, Economou A (2017) Preprotein conformational dynamics drive bivalent translocase docking and secretion. *Structure* 25: 1056–1067.e1056
11. Tsirigotaki A, Chatzi KE, Koukaki M, De Geyter J, Portaliou AG, Orfanoudaki G, Sardis MF, Trelle MB, Jorgensen TJD, Karamanou S et al (2018) Long-lived folding intermediates predominate the targeting-competent secretome. *Structure* 26: 695–707.e695
12. Zhou J, Dunker AK (2018) Regulating protein function by delayed folding. *Structure* 26: 679–681
13. Orfanoudaki G, Markaki M, Chatzi K, Tsamardinos I, Economou A (2017) MatureP: prediction of secreted proteins with exclusive information from their mature regions. *Sci Rep* 7: 3263
14. Park S, Liu G, Topping TB, Cover WH, Randall LL (1988) Modulation of folding pathways of exported proteins by the leader sequence. *Science* 239: 1033–1035
15. Beena K, Udgaonkar JB, Varadarajan R (2004) Effect of signal peptide on the stability and folding kinetics of maltose binding protein. *Biochemistry* 43: 3608–3619
16. Saio T, Guan X, Rossi P, Economou A, Kalodimos CG (2014) Structural basis for protein antiaggregation activity of the trigger factor chaperone. *Science* 344: 1250494
17. Hartl FU, Bracher A, Hayer-Hartl M (2011) Molecular chaperones in protein folding and proteostasis. *Nature* 475: 324–332
18. Hegde RS, Bernstein HD (2006) The surprising complexity of signal sequences. *Trends Biochem Sci* 31: 563–571
19. Bechtluft P, van Leeuwen RG, Tyreman M, Tomkiewicz D, Nouwen N, Tepper HL, Driessen AJ, Tans SJ (2007) Direct observation of chaperone-induced changes in a protein folding pathway. *Science* 318: 1458–1461
20. Derman AI, Puziss JW, Bassford PJ Jr, Beckwith J (1993) A signal sequence is not required for protein export in *prfA* mutants of *Escherichia coli*. *EMBO J* 12: 879–888
21. Prinz WA, Spiess C, Ehrmann M, Schierle C, Beckwith J (1996) Targeting of signal sequenceless proteins for export in *Escherichia coli* with altered protein translocase. *EMBO J* 15: 5209–5217
22. Ullers RS, Ang D, Schwager F, Georgopoulos C, Genevoux P (2007) Trigger Factor can antagonize both SecB and DnaK/DnaJ chaperone functions in *Escherichia coli*. *Proc Natl Acad Sci USA* 104: 3101–3106
23. Chatzi KE, Sardis MF, Karamanou S, Economou A (2013) Breaking on through to the other side: protein export through the bacterial Sec system. *Biochem J* 449: 25–37
24. Sala A, Bordes P, Genevoux P (2014) Multitasking SecB chaperones in bacteria. *Front Microbiol* 5: 666
25. Randall LL, Crane JM, Liu G, Hardy SJ (2004) Sites of interaction between SecA and the chaperone SecB, two proteins involved in export. *Protein Sci* 13: 1124–1133
26. Castanie-Cornet MP, Bruel N, Genevoux P (2014) Chaperone networking facilitates protein targeting to the bacterial cytoplasmic membrane. *Biochim Biophys Acta* 1843: 1442–1456
27. Hoffmann A, Bukau B, Kramer G (2010) Structure and function of the molecular chaperone Trigger Factor. *Biochim Biophys Acta* 1803: 650–661
28. Crooke E, Guthrie B, Lecker S, Lill R, Wickner W (1988) ProOmpA is stabilized for membrane translocation by either purified *E. coli* trigger factor or canine signal recognition particle. *Cell* 54: 1003–1011
29. Lecker S, Lill R, Ziegelhoffer T, Georgopoulos C, Bassford PJ Jr, Kumamoto CA, Wickner W (1989) Three pure chaperone proteins of *Escherichia coli*—SecB, trigger factor and GroEL—form soluble complexes with precursor proteins *in vitro*. *EMBO J* 8: 2703–2709
30. Niwa T, Kanamori T, Ueda T, Taguchi H (2012) Global analysis of chaperone effects using a reconstituted cell-free translation system. *Proc Natl Acad Sci USA* 109: 8937–8942
31. Bakshi S, Siryaporn A, Goulian M, Weisshaar JC (2012) Superresolution imaging of ribosomes and RNA polymerase in live *Escherichia coli* cells. *Mol Microbiol* 85: 21–38
32. Bornemann T, Holtkamp W, Wintermeyer W (2014) Interplay between trigger factor and other protein biogenesis factors on the ribosome. *Nat Commun* 5: 4180
33. Kaiser CM, Chang HC, Agashe VR, Lakshminpathy SK, Etchells SA, Hayer-Hartl M, Hartl FU, Barral JM (2006) Real-time observation of trigger factor function on translating ribosomes. *Nature* 444: 455–460
34. Merz F, Boehringer D, Schaffitzel C, Preissler S, Hoffmann A, Maier T, Rutkowska A, Lozza J, Ban N, Bukau B et al (2008) Molecular mechanism and structure of Trigger Factor bound to the translating ribosome. *EMBO J* 27: 1622–1632
35. Patzelt J, Rudiger S, Brehmer D, Kramer G, Vorderwulbecke S, Schaffitzel E, Waitz A, Hesterkamp T, Dong L, Schneider-Mergener J et al (2001) Binding specificity of *Escherichia coli* trigger factor. *Proc Natl Acad Sci USA* 98: 14244–14249

36. Ariosa A, Lee JH, Wang S, Saraogi I, Shan SO (2015) Regulation by a chaperone improves substrate selectivity during cotranslational protein targeting. *Proc Natl Acad Sci USA* 112: E3169–E3178
37. Singh R, Kraft C, Jaiswal R, Sejwal K, Kasaragod VB, Kuper J, Burger J, Mielke T, Luirink J, Bhushan S (2014) Cryo-electron microscopic structure of SecA protein bound to the 70S ribosome. *J Biol Chem* 289: 7190–7199
38. Huber D, Jamshad M, Hanmer R, Schibich D, Doring K, Marcomini I, Kramer G, Bukau B (2017) SecA cotranslationally interacts with nascent substrate proteins *in vivo*. *J Bacteriol* 199: e00622-16
39. Crooke E, Wickner W (1987) Trigger factor: a soluble protein that folds pro-OmpA into a membrane-assembly-competent form. *Proc Natl Acad Sci USA* 84: 5216–5220
40. Guthrie B, Wickner W (1990) Trigger factor depletion or overproduction causes defective cell division but does not block protein export. *J Bacteriol* 172: 5555–5562
41. Bechtluft P, Nouwen N, Tans SJ, Driessen AJ (2010) SecB—a chaperone dedicated to protein translocation. *Mol Biosyst* 6: 620–627
42. Huang C, Rossi P, Saio T, Kalodimos CG (2016) Structural basis for the antifolding activity of a molecular chaperone. *Nature* 537: 202–206
43. Fekkes P, van der Does C, Driessen AJ (1997) The molecular chaperone SecB is released from the carboxy-terminus of SecA during initiation of precursor protein translocation. *EMBO J* 16: 6105–6113
44. Hartl FU, Lecker S, Schiebel E, Hendrick JP, Wickner W (1990) The binding cascade of SecB to SecA to SecY/E mediates preprotein targeting to the *E. coli* plasma membrane. *Cell* 63: 269–279
45. Baars L, Ytterberg AJ, Drew D, Wagner S, Thilo C, van Wijk KJ, de Gier JW (2006) Defining the role of the *Escherichia coli* chaperone SecB using comparative proteomics. *J Biol Chem* 281: 10024–10034
46. Ullers RS, Luirink J, Harms N, Schwager F, Georgopoulos C, Genevaux P (2004) SecB is a bona fide generalized chaperone in *Escherichia coli*. *Proc Natl Acad Sci USA* 101: 7583–7588
47. Fan D, Liu L, Zhu L, Peng F, Zhou Q, Liu C (2017) Global analysis of the impact of deleting trigger factor on the transcriptome profile of *Escherichia coli*. *J Cell Biochem* 118: 141–153
48. Calloni G, Chen T, Schermann SM, Chang HC, Genevaux P, Agostini F, Tartaglia GG, Hayer-Hartl M, Hartl FU (2012) DnaK functions as a central hub in the *E. coli* chaperone network. *Cell Rep* 1: 251–264
49. Wang S, Yang CI, Shan SO (2017) SecA mediates cotranslational targeting and translocation of an inner membrane protein. *J Cell Biol* 216: 3639–3653
50. Lee HC, Bernstein HD (2002) Trigger factor retards protein export in *Escherichia coli*. *J Biol Chem* 277: 43527–43535
51. Saio T, Kawagoe S, Ishimori K, Kalodimos CG (2018) Oligomerization of a molecular chaperone modulates its activity. *Elife* 7: e35731
52. Hoffmann A, Becker AH, Zachmann-Brand B, Deuerling E, Bukau B, Kramer G (2012) Concerted action of the ribosome and the associated chaperone trigger factor confines nascent polypeptide folding. *Mol Cell* 48: 63–74
53. Liu CP, Perrett S, Zhou JM (2005) Dimeric trigger factor stably binds folding-competent intermediates and cooperates with the DnaK-DnaJ-GrpE chaperone system to allow refolding. *J Biol Chem* 280: 13315–13320
54. Bechtluft P, Kedrov A, Slotboom DJ, Nouwen N, Tans SJ, Driessen AJ (2010) Tight hydrophobic contacts with the SecB chaperone prevent folding of substrate proteins. *Biochemistry* 49: 2380–2388
55. Lecker SH, Driessen AJ, Wickner W (1990) ProOmpA contains secondary and tertiary structure prior to translocation and is shielded from aggregation by association with SecB protein. *EMBO J* 9: 2309–2314
56. Kleinschmidt JH (2003) Membrane protein folding on the example of outer membrane protein A of *Escherichia coli*. *Cell Mol Life Sci* 60: 1547–1558
57. Bukau B, Deuerling E, Pfund C, Craig EA (2000) Getting newly synthesized proteins into shape. *Cell* 101: 119–122
58. Gouridis G, Karamanou S, Koukaki M, Economou A (2010) *In vitro* assays to analyze translocation of the model secretory preprotein alkaline phosphatase. *Methods Mol Biol* 619: 157–172
59. Maier R, Eckert B, Scholz C, Lilie H, Schmid FX (2003) Interaction of trigger factor with the ribosome. *J Mol Biol* 326: 585–592
60. Tsirigotaki A, Papanastasiou M, Trelle MB, Jorgensen TJ, Economou A (2017) Analysis of translocation-competent secretory proteins by HDX-MS. *Methods Enzymol* 586: 57–83
61. Gouridis G, Karamanou S, Gelis I, Kalodimos CG, Economou A (2009) Signal peptides are allosteric activators of the protein translocase. *Nature* 462: 363–367
62. Gelis I, Bonvin AM, Keramisanou D, Koukaki M, Gouridis G, Karamanou S, Economou A, Kalodimos CG (2007) Structural basis for signal-sequence recognition by the translocase motor SecA as determined by NMR. *Cell* 131: 756–769
63. Breukink E, Nouwen N, van Raalte A, Mizushima S, Tommassen J, de Kruijff B (1995) The C terminus of SecA is involved in both lipid binding and SecB binding. *J Biol Chem* 270: 7902–7907
64. Hunt JF, Weinkauff S, Henry L, Fak JJ, McNicholas P, Oliver DB, Deisenhofer J (2002) Nucleotide control of interdomain interactions in the conformational reaction cycle of SecA. *Science* 297: 2018–2026
65. Karamanou S, Sianidis G, Gouridis G, Pozidis C, Papanikolaou Y, Papanikou E, Economou A (2005) *Escherichia coli* SecA truncated at its termini is functional and dimeric. *FEBS Lett* 579: 1267–1271
66. Wegrzyn RD, Deuerling E (2005) Molecular guardians for newborn proteins: ribosome-associated chaperones and their role in protein folding. *Cell Mol Life Sci* 62: 2727–2738
67. Ries F, Carius Y, Rohr M, Gries K, Keller S, Lancaster CRD, Willmund F (2017) Structural and molecular comparison of bacterial and eukaryotic trigger factors. *Sci Rep* 7: 10680
68. Bowers CW, Lau F, Silhavy TJ (2003) Secretion of LamB-LacZ by the signal recognition particle pathway of *Escherichia coli*. *J Bacteriol* 185: 5697–5705
69. Oh E, Becker AH, Sandikci A, Huber D, Chaba R, Gloge F, Nichols RJ, Typas A, Gross CA, Kramer G et al (2011) Selective ribosome profiling reveals the cotranslational chaperone action of trigger factor *in vivo*. *Cell* 147: 1295–1308
70. Papanastasiou M, Orfanoudaki G, Koukaki M, Kountourakis N, Sardis MF, Aivaliotis M, Karamanou S, Economou A (2013) The *Escherichia coli* peripheral inner membrane proteome. *Mol Cell Proteomics* 12: 599–610
71. Reusch RN (2012) Insights into the structure and assembly of *Escherichia coli* outer membrane protein A. *FEBS J* 279: 894–909
72. de Keyzer J, van der Does C, Kloosterman TG, Driessen AJ (2003) Direct demonstration of ATP-dependent release of SecA from a translocating preprotein by surface plasmon resonance. *J Biol Chem* 278: 29581–29586
73. Teter SA, Houry WA, Ang D, Tradler T, Rockabrand D, Fischer G, Blum P, Georgopoulos C, Hartl FU (1999) Polypeptide flux through bacterial Hsp70: DnaK cooperates with trigger factor in chaperoning nascent chains. *Cell* 97: 755–765
74. Arifuzzaman M, Maeda M, Itoh A, Nishikata K, Takita C, Saito R, Ara T, Nakahigashi K, Huang HC, Hirai A et al (2006) Large-scale identification of protein-protein interaction of *Escherichia coli* K-12. *Genome Res* 16: 686–691

75. Eser M, Ehrmann M (2003) SecA-dependent quality control of intracellular protein localization. *Proc Natl Acad Sci USA* 100: 13231–13234
76. Nishiyama K, Tokuda H (2010) Preparation of a highly translocation-competent proOmpA/SecB complex. *Protein Sci* 19: 2402–2408
77. Zhou Q, Sun S, Tai P, Sui SF (2012) Structural characterization of the complex of SecB and metallothionein-labeled proOmpA by cryo-electron microscopy. *PLoS One* 7: e47015
78. Tang YC, Chang HC, Roeben A, Wischnewski D, Wischnewski N, Kerner MJ, Hartl FU, Hayer-Hartl M (2006) Structural features of the GroEL-GroES nano-cage required for rapid folding of encapsulated protein. *Cell* 125: 903–914
79. Clerico EM, Tilitsky JM, Meng W, Gierasch LM (2015) How hsp70 molecular machines interact with their substrates to mediate diverse physiological functions. *J Mol Biol* 427: 1575–1588
80. Vandenberk N, Karamanou S, Portaliou AG, Zorzini V, Hofkens J, Hendrix J, Economou A (2019) The preprotein binding domain of SecA displays intrinsic rotational dynamics. *Structure* 27: 90–101.e106
81. Ernst I, Haase M, Ernst S, Yuan S, Kuhn A, Leptihn S (2018) Large conformational changes of a highly dynamic pre-protein binding domain in SecA. *Commun Biol* 1: 130
82. Oliver DB, Cabelli RJ, Dolan KM, Jarosik GP (1990) Azide-resistant mutants of *Escherichia coli* alter the SecA protein, an azide-sensitive component of the protein export machinery. *Proc Natl Acad Sci USA* 87: 8227–8231
83. Paetzel M (2014) Structure and mechanism of *Escherichia coli* type I signal peptidase. *Biochim Biophys Acta* 1843: 1497–1508
84. Chang CN, Blobel G, Model P (1978) Detection of prokaryotic signal peptidase in an *Escherichia coli* membrane fraction: endoproteolytic cleavage of nascent f1 pre-coat protein. *Proc Natl Acad Sci USA* 75: 361–365
85. Gouridis G, Karamanou S, Sardis MF, Schärer MA, Capitani G, Economou A (2013) Quaternary dynamics of the SecA motor drive translocase catalysis. *Mol Cell* 52: 655–666
86. Karamanou S, Vrontou E, Sianidis G, Baud C, Roos T, Kuhn A, Politou AS, Economou A (1999) A molecular switch in SecA protein couples ATP hydrolysis to protein translocation. *Mol Microbiol* 34: 1133–1145
87. Sianidis G, Karamanou S, Vrontou E, Boulias K, Repanas K, Kyrpidis N, Politou AS, Economou A (2001) Cross-talk between catalytic and regulatory elements in a DEAD motor domain is essential for SecA function. *EMBO J* 20: 961–970
88. Wowor AJ, Yan Y, Auclair SM, Yu D, Zhang J, May ER, Gross ML, Kendall DA, Cole JL (2014) Analysis of SecA dimerization in solution. *Biochemistry* 53: 3248–3260